Toward Metal-Capped One-Dimensional Carbon Allotropes: Wirelike C_6-C_{20} Polyynediyl Chains That Span Two Redox-Active (η^5-C_5Me_5)Re(NO)(PPh_3) Endgroups

Roman Dembinski,[1a] Tamás Bartik,[1a] Berit Bartik,[1a] Monika Jaeger,[1a,b] and J. A. Gladysz*[1a,c]

Contribution from the Department of Chemistry, University of Utah, Salt Lake City, Utah 84112, and Institut für Organische Chemie, Friedrich-Alexander Universität Erlangen-Nürnberg, Henkestrasse 42, 91054 Erlangen, Germany

Received August 2, 1999

Abstract: Reaction of the butadiynyl complex (η^5-C_5Me_5)Re(NO)(PPh_3)(C≡CC≡CH) (**ReC$_4$H**) with Cu(OAc)$_2$ (pyridine, 80 °C) gives the μ-octatetraynediyl complex **ReC$_8$Re** (70%). Analogous cross-coupling of **ReC$_4$H** and **ReC$_2$H** gives (after chromatography) **ReC$_4$Re** (14%), **ReC$_6$Re** (44%), and **ReC$_8$Re** (15%). Longer sp carbon chains are accessed by reactions of **ReC$_4$H** with *n*-BuLi and CuI, which give **ReC$_4$Cu**. This isolable species is treated in situ with BrC≡CSiEt$_3$ or BrC≡CC≡CSiMe$_3$ (excess $EtNH_2$, THF) to give **ReC$_6$SiEt$_3$** or **ReC$_8$SiMe$_3$** (84−77%). Desilylations (wet *n*-$Bu_4N^+F^-$) yield **ReC$_6$H** or **ReC$_8$H** (88−73%). Then Cu(OAc)$_2$ (pyridine, 50 °C) gives **ReC$_{12}$Re** or **ReC$_{16}$Re** (71−67%). The former is also available from **ReC$_4$Cu** and BrC≡CC≡CBr (45%), and **ReC$_{10}$Re** can be accessed by cross-coupling. **ReC$_6$H** and **ReC$_8$H** are similarly converted to **ReC$_{10}$SiR$_3$** (R = Me, Et; 51−26%) and **ReC$_{12}$SiMe$_3$** (43%). Desilylation of **ReC$_{10}$SiR$_3$** gives labile **ReC$_{10}$H**, but only black powder is obtained from **ReC$_{12}$SiMe$_3$**. In situ coupling of **ReC$_{10}$H** gives **ReC$_{20}$Re** (52−34%), which unlike lower homologues is not obtained in analytically pure form. The effects of chain length upon visible spectra (progressively red-shifted and more intense bands; ϵ >190 000 M^{-1} cm^{-1}), IR/Raman $\nu_{C\equiv C}$ patterns (progressively more bands), ^{13}C NMR chemical shifts (asymptotic limit of 64−67 ppm for ReC≡C(C≡C)$_n$), cyclic voltammetry (decreased reversibility of two oxidations; a gradual shift of the first to thermodynamically less favorable potentials, so that only a single oxidation is observed for **ReC$_{20}$Re**), and thermal stabilities (solid-state decompositions at 155 °C, **ReC$_{20}$Re**, and 178−217 °C, lower homologues) are studied in detail.

Compounds in which unsaturated elemental carbon chains span two metals, $L_mMC_xM'L'_{m'}$ (**I**; Scheme 1),[2] constitute the most fundamental class of carbon-based molecular wires.[3] Such one-dimensional assemblies must by definition be composed only of sp-hybridized carbon. They bear an obvious conceptual relationship to the classic two- and three-dimensional polymeric carbon allotropes, graphite and diamond, which are based upon sp^2- and sp^3-hybridized carbon.[4] Importantly, all of these species must terminate with a non-carbon atom or some entity that differs from the repeat unit. Hence, at very high chain lengths, **I** can be viewed as a genuine carbon allotrope.

The polymeric sp carbon allotrope is often referred to as "carbyne", and numerous syntheses have been claimed.[5,6] However, most samples are intractable or difficult to characterize. As shown in Scheme 1, different valence structures are possible. One features alternating triple and single bonds (alkynyl or polyynediyl), with sp carbon termini bearing *one endgroup* X (**II**). Another consists solely of double bonds (cumulenic), with sp^2 carbon termini bearing *two endgroups* X (**III**). In the case of sp^3 carbon termini with *three endgroups* X (**IV**), the bond order pattern of **II** is reversed. These distinctions become important when the X_n moieties are collectively replaced by a single redox-active metal capable of forming one, two, or three bonds to carbon.

Scheme 1. Carbon Chain Compounds

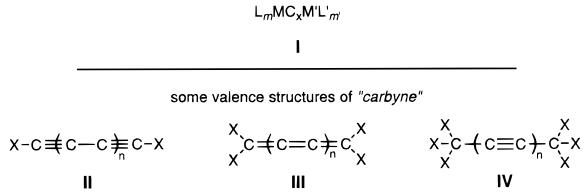

(1) (a) University of Utah. (b) Formerly Monika Brady. (c) Friedrich-Alexander Universität Erlangen-Nürnberg. Address correspondence to this address.

(2) General reviews or accounts: (a) Lang, H. *Angew. Chem.* **1994**, *106*, 569; *Angew. Chem., Int. Ed. Engl.* **1994**, *33*, 547. (b) Bunz, U. *Angew. Chem.* **1996**, *108*, 1047; *Angew. Chem., Int. Ed. Engl.* **1996**, *35*, 969. (c) Bruce, M. I. *Coord. Chem. Rev.* **1997**, *166*, 91. (d) Paul, F.; Lapinte, C. *Coord. Chem. Rev.* **1998**, *178−180*, 427.

(3) (a) Ward, M. D. *Chem. Ind.* **1997**, 640. (b) Astruc, D. *Acc. Chem. Res.* **1997**, *30*, 383. (c) Swager, T. M. *Acc. Chem. Res.* **1998**, *31*, 201. (d) Creager, S.; Yu, C. J.; Bamdad, C.; O'Connor, S.; MacLean, T.; Lam, E.; Chong, Y.; Olsen, G. T.; Luo, J.; Gozin, M.; Kayyem, J. F. *J. Am. Chem. Soc.* **1999**, *121*, 1059.

(4) Henning, T.; Salama, F. *Science* **1998**, *282*, 2204.

(5) Reviews and critical analyses: (a) Mel'nichenko, V. M.; Sladkov, A. M.; Nikulin, Yu. N. *Russ. Chem. Rev.* **1982**, *51*, 421. (b) Smith, P. P. K.; Buseck, P. R. *Science* **1982**, *216*, 984. (c) Heimann, R. B. *Diamond Relat. Mater.* **1994**, *3*, 1151. (d) Kudryavtsev, Yu. P.; Evsyukov, S.; Guseva, M.; Babaev, V.; Khvostov, V. In *Chemistry and Physics of Carbon*; Thrower, P. A., Ed.; Marcel Dekker: New York, 1997; Vol. 25, pp 1−69.

(6) Lagow, R. J.; Kampa, J. J.; Wei, H.-C.; Battle, S. L.; Genge, J. W.; Laude, D. A.; Harper, C. J.; Bau, R.; Stevens, R. C.; Haw, J. F.; Munson, E. *Science* **1995**, *267*, 362.

10.1021/ja992747z CCC: $19.00
Published on Web 01/21/2000

There is a fascinating older literature involving polyynes with bulky endgroups.[7−9] For example, *tert*-butyl-capped species $Me_3C(C{\equiv}C)_nCMe_3$ (n = 4−8, 10, 12) have been prepared by classical techniques and characterized by UV−visible spectra and melting points.[7] Similar $R_3Si(C{\equiv}C)_nSiR_3$ species have been reported (n = 4−10, 12, 16), but the higher oligomers were generated in solution, characterized by UV−visible spectra, and not purified further.[8] The physical properties of both series remain to be probed by modern methods. More recently, Hirsch et al. have prepared mixtures of cyano-capped species $NC(C{\equiv}C)_nCN$ (n = 3−8) by graphite vapor deposition, and following HPLC separation carefully documented their properties.[10] Lagow et al. have claimed similar syntheses of higher oligomers (n = 35−75) with cyano and trifluoromethyl endgroups.[6] However, systems with smaller endgroups are generally less stable and often explosive. Cumulated species (**III**) also appear to be less stable. Isolable examples are so far limited to C_6 chains (n = 2).[11]

Complexes of the type **I** have attracted the attention of numerous researchers from the standpoints of fundamental physical and chemical properties, materials attributes, molecular electronics, and catalysis, as summarized in reviews[2] and previous full papers in this series.[12,13] In this paper, we describe the systematic synthesis and detailed physical characterization of C_6−C_{20} polyynes with the chiral rhenium endgroup (η^5-C_5Me_5)Re(NO)(PPh_3) (**Re**). This constitutes, together with the work of Hirsch et al. noted above, the first modern investigation of a homologous series of long polyynes. We carefully document the effect of chain length upon the IR, Raman, ^{13}C NMR, and UV−visible spectra, as well as redox potentials and thermal stabilities. Portions of this work have been communicated.[14,15]

Other important background details are as follows. In a previous full paper,[12] we described the isolation and physical properties of the three "consanguineous" or redox-related C_4 complexes $\mathbf{ReC_4Re}^{n+}n(PF_6^-)$ shown in Scheme 2. This illustrates the interconversion of neutral polyynediyl and dicationic cumulenic valence structures, and the electrochemical generation of higher homologues is described below. Related FeC_4Fe, RuC_4Ru, and MnC_4Mn species, some of which can be even further oxidized, have been characterized by Lapinte, Bruce, and Berke.[16−18] Some partially characterized C_6 and C_8 complexes of the type **I** had been reported at the outset of this work.[19] Additional examples are now available,[20−23] the most noteworthy of which is an FeC_8Fe system of Lapinte that can be isolated in both neutral octatetraynediyl and radical cation oxidation states.[16d] Outside of the title compounds, only two other complexes with longer chains (C_{12}) have been described to date.[21b,23]

Scheme 2. Interconversion of the C_4 Complexes $\mathbf{ReC_4Re}^{n+}n(PF_6^-)$

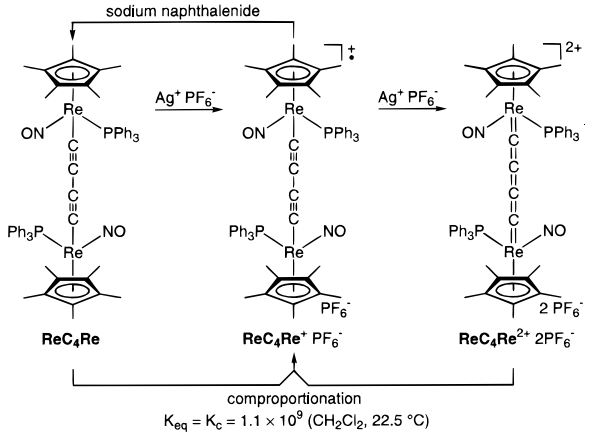

Results

1. C_6 and C_8 Complexes. We first sought an efficient route to the octatetraynediyl complex $\mathbf{ReC_8Re}$, and we attempted a synthesis analogous to that of $\mathbf{ReC_4Re}$ (Scheme 2).[12] This employed the racemic butadiynyl complex (η^5-C_5Me_5)Re(NO)(PPh_3)(C≡CC≡CH) ($\mathbf{ReC_4H}$), which is available in three steps and 75−81% overall yields via a sequence that starts with the methyl complex **ReMe** and $HC{\equiv}CC{\equiv}CSiMe_3$.[13a] As shown in Scheme 3, oxidative coupling with $Cu(OAc)_2$ (1.5 equiv) in pyridine at 80 °C gave $\mathbf{ReC_8Re}$ in 70% yield as an air-stable orange powder.[24]

We next sought homologues with odd numbers of alkyne linkages. Accordingly, a 50:50 mixture of $\mathbf{ReC_4H}$ and $\mathbf{ReC_2H}$[25] was similarly combined with $Cu(OAc)_2$ in pyridine (Scheme 3). Subsequent silica gel column chromatography easily separated the desired cross-coupling product, hexatriynediyl complex $\mathbf{ReC_6Re}$ (44%), from smaller amounts of the homocoupling products $\mathbf{ReC_4Re}$ (14%) and $\mathbf{ReC_8Re}$ (15%). The order of

(7) (a) Jones, E. R. H.; Lee, H. H.; Whiting, M. C. *J. Chem. Soc.* **1960**, 3483. (b) Johnson, T. R.; Walton, D. R. M. *Tetrahedron* **1972**, *28*, 5221.

(8) Eastmond, R.; Johnson, T. R.; Walton, D. R. M. *Tetrahedron* **1972**, *28*, 4601.

(9) (a) Bohlmann, F. *Angew. Chem.* **1953**, *65*, 385. (b) Sladkov, A. M.; Kudryavtsev, Yu. P. *Russian Chem. Rev.* **1963**, *32*, 229.

(10) (a) Schermann, G.; Grösser, T.; Hampel, F.; Hirsch, A. *Chem. Eur. J.* **1997**, *3*, 1105. (b) Schermann, G. Ph.D. Thesis, Universität Erlangen-Nürnberg, 1999.

(11) Bildstein, B.; Schweiger, M.; Angleitner, H.; Kopacka, H.; Wurst, K.; Ongania, K.-H.; Fontani, M.; Zanello, P. *Organometallics* **1999**, *18*, 4286 and references therein.

(12) Brady, M.; Weng, W.; Zhou, Y.; Seyler, J. W.; Amoroso, A. J.; Arif, A. M.; Böhme, M.; Frenking, G.; Gladysz, J. A. *J. Am. Chem. Soc.* **1997**, *119*, 775.

(13) (a) Weng, W.; Bartik, T.; Brady, M.; Bartik, B.; Ramsden, J. A.; Arif, A. M.; Gladysz, J. A. *J. Am. Chem. Soc.* **1995**, *117*, 11922. (b) Falloon, S. B.; Szafert, S.; Arif, A. M.; Gladysz, J. A. *Chem. Eur. J.* **1998**, *4*, 1033. (c) Bartik, T.; Weng, W.; Ramsden, J. A.; Szafert, S.; Falloon, S. B.; Arif, A. M.; Gladysz, J. A. *J. Am. Chem. Soc.* **1998**, *120*, 11071.

(14) (a) Brady, M.; Weng, W.; Gladysz, J. A. *J. Chem. Soc., Chem. Commun.* **1994**, 2655. (b) Bartik, T.; Bartik, B.; Brady, M.; Dembinski, R.; Gladysz, J. A. *Angew. Chem.* **1996**, *108*, 467; *Angew. Chem., Int. Ed. Engl.* **1996**, *35*, 414.

(15) Some sp carbon/sp carbon bond-forming reactions are detailed in the following notes: (a) Bartik, B.; Dembinski, R.; Bartik, T.; Arif, A. M.; Gladysz, J. A. *New J. Chem.* **1997**, *21*, 739. (b) Dembinski, R.; Lis, T.; Szafert, S.; Mayne, C. L.; Bartik, T.; Gladysz, J. A. *J. Organomet. Chem.* **1999**, *578*, 229.

(16) (a) Le Narvor, N.; Toupet, L.; Lapinte, C. *J. Am. Chem. Soc.* **1995**, *117*, 7129. (b) Coat, F.; Guillevic, M.-A.; Toupet, L.; Paul, F.; Lapinte, C. *Organometallics* **1997**, *16*, 5988. (c) Le Narvor, N.; Lapinte, C. *C. R. Acad. Sci. Paris, Ser. IIc* **1998**, 745. (d) Guillemot, M.; Toupet, L.; Lapinte, C. *Organometallics* **1998**, *17*, 1928.

(17) (a) Bruce, M. I.; Denisovich, L. I.; Low, P. J.; Peregudova, S. M.; Ustynyuk, N. A. *Mendeleev Commun.* **1996**, 200. (b) Bruce, M. I.; Low, P. J.; Costuas, K.; Halet, J.-F.; Best, S. P.; Heath, G. A. *J. Am. Chem. Soc.* **2000**, *122*, in press.

(18) Kheradmandan, S.; Heinze, K.; Schmalle, H. W.; Berke, H. *Angew. Chem.* **1999**, *111*, 2412; *Angew. Chem., Int. Ed.* **1999**, *38*, 2270.

(19) Kim, P. J.; Masai, H.; Sonogashira, K.; Hagihara, N. *Inorg. Nucl. Chem. Lett.*, **1970**, *6*, 181.

(20) Coat, F.; Lapinte, C. *Organometallics* **1996**, *15*, 477.

(21) (a) Akita, M.; Chung, M.-C.; Sakurai, A.; Sugimoto, S.; Terada, M.; Tanaka, M.; Moro-oka, Y. *Organometallics* **1997**, *16*, 4882. (b) Sakurai, A.; Akita, M.; Moro-oka, Y. *Organometallics* **1999**, *18*, 3241.

(22) (a) Bruce, M. I.; Ke, M.; Low, P. J.; Skelton, B. W.; White, A. H. *Organometallics* **1998**, *17*, 3539. (b) Bruce, M. I.; Kelly, B. D.; Skelton, B. W.; White, A. H. *J. Chem. Soc., Dalton Trans.* **1999**, 847.

(23) Peters, T. B.; Bohling, J. C.; Arif, A. M.; Gladysz, J. A. *Organometallics* **1999**, *18*, 3261.

(24) Alternatively, $\mathbf{ReC_8Re}$ can be obtained in quantitative NMR yield from *trans*-$\mathbf{ReC_4Pd(PEt_3)_2C_4Re}$[13a] in refluxing benzene. We thank Dr. Arturo Casado for this observation.

(25) Ramsden, J. A.; Weng, W.; Gladysz, J. A. *Organometallics* **1992**, *11*, 3635.

Scheme 3. Homocoupling and Cross-Coupling of the Butadiynyl Complex **ReC$_4$H**

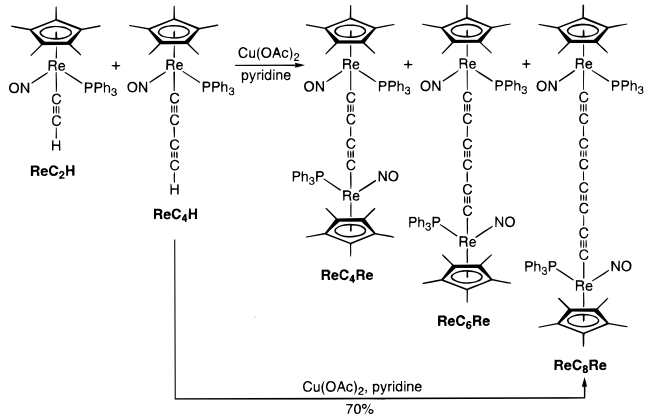

elution paralleled the absolute solubilities (lower with longer chain length). More convergent approaches to **ReC$_6$Re** were not successful.[26]

The new complexes **ReC$_6$Re** and **ReC$_8$Re**, and all higher homologues, were characterized by IR, Raman, NMR, and UV−visible spectroscopy, cyclic voltammetry (CV),[27] differential scanning calorimetry (DSC),[28] mass spectrometry, and microanalysis. Key data are summarized in Tables 1 and 2 and Figures 1−4, and representative IR and Raman spectra are reproduced in the Supporting Information. Special features of interest include the effect of chain length upon (1) IR and Raman $\nu_{C\equiv C}$ patterns, (2) ^{13}C NMR chemical shifts, (3) colors and visible absorptions, (4) redox potentials, and (5) thermal stabilities. Trends are analyzed in detail in the Discussion section.

Since racemic monorhenium educts are used in Scheme 3, the dirhenium products should be mixtures of *meso* and *dl* diastereomers. Low-temperature ^{13}C and ^{31}P NMR spectra of **ReC$_6$Re** showed two closely spaced sets of signals (50:50), consistent with this premise. However, **ReC$_8$Re** gave a single set of NMR signals under all conditions assayed, presumably due to the greater distance between stereocenters.[29] The diastereomers of **ReC$_4$Re** separate by crystallization, but all attempts to obtain enriched samples of **ReC$_6$Re** or **ReC$_8$Re**, including analytical HPLC, were unsuccessful. Accordingly, the title compounds were characterized as mixtures of diastereomers. Importantly, the diastereomers of **ReC$_4$Re**$^{n+}n(PF_6^-)$ give identical IR, UV−visible, CV, and ESR data.[12] Hence, these properties are not sensitive to the relative rhenium configurations.

Another strategy for diastereomerically pure **ReC$_8$Re** would utilize enantiomerically pure **ReC$_4$H**. The precursor **ReMe** is available in resolved form,[30] and a parallel sequence was conducted. Unfortunately, methods to assay the enantiomeric purities of the resulting **ReC$_4$SiMe$_3$**, **ReC$_4$H**, or **ReC$_8$Re** (which were optically active) could not be found.[31,32] The last gave crystals marginally suitable for X-ray analysis, but the structure did not refine satisfactorily. Although the metrical parameters are not usable, an ORTEP diagram is given in Figure 5, together with that of **ReC$_4$Re** obtained earlier.[12] This shows that the carbon chain is much more exposed in **ReC$_8$Re** than in **ReC$_4$Re**, and it would logically undergo bimolecular reactions more rapidly. Despite extensive efforts, we were unable to grow X-ray quality single crystals of any other dirhenium complex in this paper. The presence of diastereomers likely contributes to this difficulty.

Table 1. Key IR and Raman Data for Polyynediyl Complexes (cm^{-1})

	IR			Raman
complex	medium	ν_{NO}	ν_{CC}	ν_{CC}[a] (CH_2Cl_2)
ReC$_4$Re[b,c]	THF	1630 s	1967 w	2056 s
	CH_2Cl_2	1623 s	1964 w	
	KBr	1629 s br	1968 w	
ReC$_6$Re	THF	1645 s	2064 m	1951 s
	CH_2Cl_2	1640 s	2061 m	2100 s
	KBr	1638 s	2058 m	
ReC$_8$Re	THF	1651 s	1956 m	2000 s
			2112 s	2100 s
	CH_2Cl_2	1648 s	1959 m	
			2108 s	
	KBr	1642 s	1954 m	
			2107 s	
ReC$_{10}$Re	THF	1649 s	2000 m	−
			2120 s	
	KBr	1647 s	1993 m	
			2114 s	
ReC$_{12}$Re	THF	1653 s	1952 s	1951 s
			2056 vs	2030 m
			2117 m	2135 w
	KBr	1653 s	1946 s	
			2050 s	
			2112 m	
ReC$_{16}$Re	THF	1654 s	1941 vs	1921 s
			2014 vs	2000 w
			2074 m	2101 vw
	KBr	1655 s	1938 s	2140 vw
			2012 s	
			2069 m	
ReC$_{20}$Re	THF	1653 s	1962 vs	1899 s
			2031 vs	1984 w
			2058 s	2068 vw
			2116 w	2102 vw
			2164 w	
	KBr	1655 s	1949 s	
			2036 s	
			2101 w	
			2136 w	

[a] Raman spectra did not show ν_{NO} bands. [b] *SS,RR* and *SR,RS* diastereomers gave identical spectra. [c] Data from ref 12.

2. C$_{10}$, C$_{12}$, and C$_{16}$ Complexes. We sought to extend the methodology in Scheme 3 to higher homologues. Thus, educts with longer C_xH chains were required. As shown in Scheme 4, **ReC$_4$H** was treated with *n*-BuLi and CuI in THF to generate an alkynyl copper species of empirical formula (η^5-C_5Me_5)Re(NO)(PPh_3)(C≡CC≡CCu) (**ReC$_4$Cu**). This useful synthon has been described in previous notes involving hexatriynyl and octatetraynyl complexes.[15] It may be isolated as a thermally

(26) The most intensive efforts involved reactions of **ReC$_2$Cu** (see higher homologues below) and IC≡CI (0.5 equiv). Other coupling methods described below and elsewhere[15b] were also unsuccessful.

(27) In response to conventions proposed in a review that appeared following our communication (Connelly, N. G.; Geiger, W. E. *Chem. Rev.* **1996**, *96*, 877), we present our CV data relative to a new $E^{o\prime}$ value for ferrocene. See also footnote 25 in ref 12.

(28) DSC parameters (Cammenga, H. K.; Epple, M. *Angew. Chem.* **1995**, *107*, 1284; *Angew. Chem., Int. Ed. Engl.* **1995**, *34*, 1171): T_i, initial peak temperature; T_e, extrapolated peak-onset temperature; T_p, maximum peak temperature.

(29) (a) Interestingly, the diastereomers of analogues with bulkier triarylphosphine ligands show separate NMR signals. (b) Meyer, W. E. Ph.D. Thesis, University of Utah, 1999.

(30) Huang, Y.-H.; Niedercorn, F.; Arif, A. M.; Gladysz, J. A. *J. Organomet. Chem.* **1990**, *383*, 213.

(31) The pentamethylcyclopentadienyl series is much more configurationally labile than the cyclopentadienyl series. For comparisons, see: (a) Peng, T.-S.; Winter, C. H.; Gladysz, J. A. *Inorg. Chem.* **1994**, *33*, 2534 and references therein. (b) Salzer, A.; Hosang, A.; Knuppertz, J.; Englert, U. *Eur. J. Inorg. Chem.* **1999**, 1497.

(32) An analogous sequence from enantiomerically pure **ReMe** to **ReC$_4$Re** gave a 70:30 mixture of *dl* and *meso* diastereomers.

Table 2. Summary of ^{13}C NMR Chemical Shifts for Polyynediyl Complexes (ppm)[a]

complex	solvent	ReC≡ [$^2J_{CP}$, Hz]	ReC≡C [$^4J_{CP}$, Hz]	other
ReC$_4$Re[b]	CD_2Cl_2[c]	96.6/96.5 [13.0/13.0][d]	116.7/ 116.5	
	THF-d_8[e]	96.4 [12.7]	116.4	
	C_6D_6[e]	95.8 [10.9]	117.5	
ReC$_6$Re	CD_2Cl_2[c]	106.8/106.5 [16.8/16.0]	112.6	65.0/64.9[d]
	THF-d_8[c]	104.2/103.3 [15.7/16.0]	114.3/ 113.9	65.7/65.2[d]
ReC$_8$Re	CD_2Cl_2	111.0 [18.4][d]	112.7	66.8 [2.9] 63.8
	THF-d_8	109.7 [16.9]	113.3	66.6 [2.7] 64.5
ReC$_{10}$Re	CD_2Cl_2	117.3 [15.7]	112.7	66.1 [2.7] 66.3, 64.1
ReC$_{12}$Re	CD_2Cl_2	116.8 [15.6]	113.7	66.0 [3.3] 67.1, 66.3, 64.4
	C_6D_6	117.6 [15.7]	114.1	66.5 [2.8] 67.4, 66.8, 66.0
ReC$_{16}$Re	CD_2Cl_2	125.1 [15.2]	113.2	66.6 [2.4] 66.7, 66.4, 65.6, 65.5, 65.2
ReC$_{20}$Re	CD_2Cl_2	127.3 [14.6][d]	113.2	66.6[d] 67.0, 66.5, 65.5, 65.4, 65.3, 64.9, 64.8

[a] Mixtures of *SS,RR* and *SR,RS* diastereomers unless noted. [b] ^{13}C labeled. [c] Some signals of the two diastereomers were resolved. [d] Due to the spectral resolution, this $^2J_{CP}$ value has a larger uncertainty, or the $^4J_{CP}$ value could not be assigned. [e] *SS,RR* diastereomer; data from ref 12.

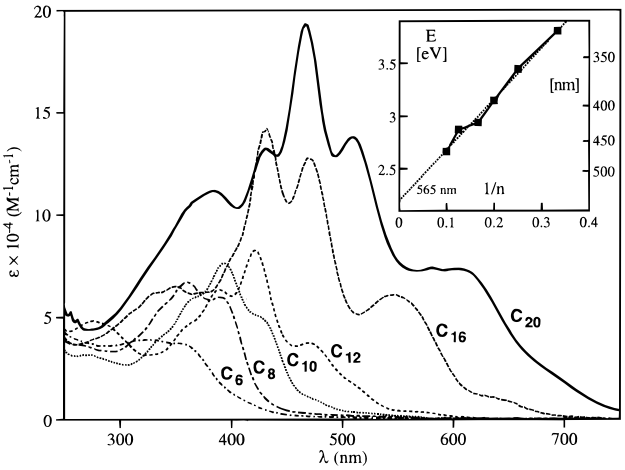

Figure 1. UV−visible spectra of polyynediyl complexes (CH_2Cl_2) and (inset) relationship between λ_{max} (eV) and $1/n$ (n = number of alkynyl units).

stable powder, but it is normally used in situ. All attempts to obtain crystals or a crystalline derivative have been unsuccessful.[33]

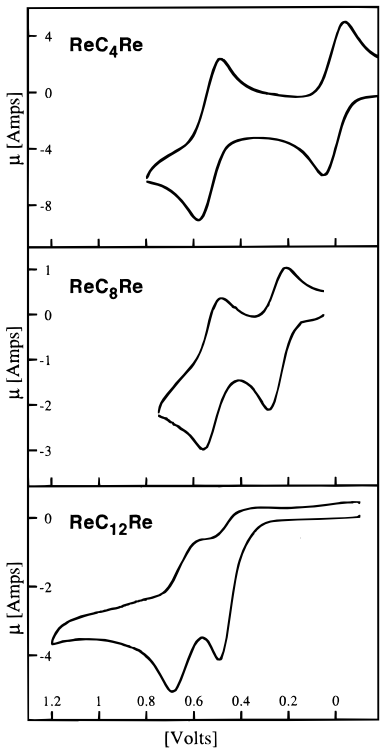

Figure 2. Representative cyclic voltammograms under the conditions of Figure 3.

The adduct **ReC$_4$Cu** can be employed in the variation of the Cadiot−Chodkiewicz reaction depicted in Scheme 4.[34] Accordingly, reactions with BrC≡CSiEt$_3$[15b] or BrC≡CC≡CSiMe$_3$[15a] in the presence of excess $EtNH_2$ (−20 °C) gave the analytically pure hexatriynyl and octatetraynyl complexes **ReC$_6$SiEt$_3$** and **ReC$_8$SiMe$_3$** in 84−77% yields after crystallization.[35] Both of these compounds have been fully described in notes,[15] including the crystal structure of the latter.[15a] Hence, optimized preparations are given in the Supporting Information, and key spectroscopic data are presented below with those of new higher homologues.

As shown in Scheme 4, **ReC$_6$SiEt$_3$** and **ReC$_8$SiMe$_3$** could easily be converted to the corresponding C_xH complexes **ReC$_6$H** and **ReC$_8$H**. The K_2CO_3/methanol recipe in our communication required 8−12 h for completion.[12,15b] That in Scheme 4, wet *n*-$Bu_4N^+F^-$/THF, requires only 0.5 h. These compounds were, unlike their precursors, moderately air sensitive as solids and more air sensitive in solution. The complex **ReC$_6$H** has also been described in a note,[15b] but for convenience the preparation is given in the Supporting Information.

As shown in Scheme 5, **ReC$_6$H** and **ReC$_8$H** were separately combined with $Cu(OAc)_2$ in pyridine at 50 °C. Workups gave the dodecahexaynediyl and hexadecaoctaynediyl complexes **ReC$_{12}$Re** and **ReC$_{16}$Re** in 71−67% yields as orange, air-stable, analytically pure powders. These were characterized analogously to the lower homologues, and data are summarized in Tables 1 and 2 and Figures 1−4. More convergent syntheses were also

(33) (a) Copper alkynyl complexes have been extensively studied (see: Janssen, M. D.; Köhler, K.; Herres, M.; Dedieu, A.; Smeets, W. J. J.; Spek, A. L.; Grove, D. M.; Lang, H.; van Koten, G. *J. Am. Chem. Soc.* **1996**, *118*, 4817 and references therein) and commonly exist as aggregates (e.g., tetramers). We speculate that the difficulty in crystallizing **ReC$_x$Cu** is due to the mixtures of diastereomers that are likely present. We have investigated polydentate ligands that are capable of binding copper and deaggregating these structures, but the adducts have so far resisted crystallization. (b) Procedures for the isolation of **ReC$_x$Cu** (x = 2, 4, 6) are given in the Supporting Information. (c) Procedures that utilize *t*-BuOCu in place of *n*-BuLi and CuI have also been developed. However, this milder base is not commercially available. These procedures are also given in the Supporting Information, except for one case where there is a distinct yield advantage.

(34) Sonogashira, K. In *Metal Catalyzed Cross-coupling Reactions*; Diederich, F., Stang, P. J., Eds.; Wiley-VCH: Weinheim, 1998; Chapter 5.2.1.

(35) The use of two different silicon endgroups reflects a variety of factors. The C_4 building block BrC≡CC≡CSiMe$_3$ is available in two easy steps from commercial Me$_3$SiC≡CC≡CSiMe$_3$,[15a] but BrC≡CC≡CSiEt$_3$ must be prepared in three steps from commercial HC≡CSiEt$_3$ (Experimental Section). On the other hand, BrC≡CSiEt$_3$ has a greater shelf stability than BrC≡CSiMe$_3$ or IC≡CSiMe$_3$, and the synthesis[15b] is less demanding. In general, SiEt$_3$ endgroups impart somewhat greater stabilities but sometimes higher solubilities than optimal for crystallizations.

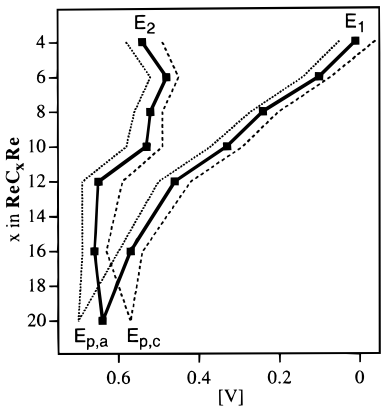

Complex	$E_{1p,a}$ $E_{2p,a}$	$E_{1p,c}$ $E_{2p,c}$	E_1 E_2	ΔE_1 ΔE_2	$i_{c/a}$[a] (K_c)[b]
	[V][d]	[V][d]	[V][d]	[mV][c]	
ReC$_4$Re	0.05	-0.04	0.01	90	1
	0.58	0.49	0.54	90	(1.1×10^9)
ReC$_6$Re	0.14	0.07	0.10	70	1
	0.52	0.45	0.48	70	(3.0×10^6)
ReC$_8$Re	0.27	0.20	0.24	70	>1
	0.56	0.49	0.52	70	(59×10^3)
ReC$_{10}$Re	0.47	0.39	0.43	80	>1
	0.68	0.59	0.63	90	(2.6×10^3)
ReC$_{12}$Re	0.50	0.42	0.46	80	>>1
	0.69	0.59	0.65	100	(1.7×10^3)
ReC$_{16}$Re	0.60	0.54	0.57	60	>>1
	0.69	0.63	0.66	60	(34)
ReC$_{20}$Re	0.70	0.57	0.64	130	>>>1

Figure 3. Cyclic voltammetry data for polyynediyl complexes. Conditions: $(7-9) \times 10^{-5}$ M in 0.1 M $Bu_4N^+BF_4^-/CH_2Cl_2$ at 22.5 ± 1 °C; Pt working and counter electrodes, potential vs Ag wire pseudo-reference; scan rate, 100 mV/s; ferrocene = 0.46 V; additional details are given in the Supporting Information. Table footnotes: [a]Improved reversibility is generally seen at lower temperatures. [b]K_c = Comproportionation constant; calculated as described in footnote 34 of ref 12. [c]Except for **ReC$_{20}$Re**, each compound exhibits two, one-electron oxidations.

probed. For example, **ReC$_4$Cu** was treated with excess $EtNH_2$ and then the *di*bromide building block BrC≡CC≡CBr.[36] Workup gave **ReC$_{12}$Re** in 45% yield. However, analogous sequences involving the tetrayne BrC≡CC≡CC≡CC≡CBr[37] were often complicated by violent detonations. In no case was any **ReC$_{16}$Re** detected.

We again sought homologues with odd numbers of alkyne linkages. Accordingly, a 50:50 mixture of **ReC$_6$SiEt$_3$** and **ReC$_4$SiMe$_3$** was converted to **ReC$_6$H** and **ReC$_4$H** (*n*-$Bu_4N^+F^-$/toluene). The sample was treated with $Cu(OAc)_2$ (pyridine, 60 °C). Unlike the case in Scheme 3, the products could be only partially separated by silica gel column chromatography. A center cut from the center band was rechromatographed to give a sufficient quantity of pure **ReC$_{10}$Re** for characterization (9% yield). Attempts to develop preparatively useful syntheses from **ReC$_4$Cu** and IC≡CI (excess $EtNH_2$, THF, −20 °C) or **ReC$_4$Li** and $[PhIC{\equiv}CIPh]^{2+}2(TfO^-)$ (THF, −80 °C) gave complex mixtures, with trace quantities of **ReC$_{10}$Re** detectable by mass spectrometry.

(36) (a) Straus, F.; Kollek, L.; Hauptmann, H. *Chem. Ber*. **1930**, *63*, 1886. This paper details the explosive properties of BrC≡CC≡CBr, as does a letter by Pettersen and Cash: Pettersen, R. C.; Cash, G. G. *Chem. Eng. News* **1977**, *55* (Nov 28), 36. (b) Heilbronner, E.; Hornung, V.; Maier, J. P.; Kloster-Jensen, E. *J. Am. Chem. Soc*. **1974**, *96*, 4252.

(37) We characterized this previously unreported compound by IR (cm^{-1}, THF, $\nu_{C\equiv C}$ 2197 vs, 2070 w), $^{13}C\{^1H\}$ NMR ($C_6D_5CD_3$, 66.3 (s, *C*CCCBr), 62.0 (s, C*C*CCBr), 59.9 (s, *C*CBr), 42.9 (s, C*C*Br)), and mass spectrometry. To avoid the ethical dilemma of reporting an extremely hazardous procedure in the open literature, we will provide synthetic details upon request to laboratories that have experience with and proper facilities for manipulating highly explosive compounds.

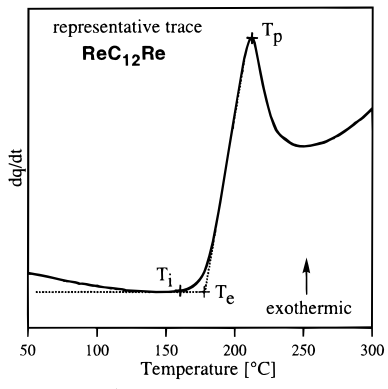

Complex	T_i	T_e	T_p	Capillary Thermolysis[a]
ReC$_4$Re	158	192	230	>250[b]
ReC$_6$Re	186	207	220	179-182 dec[c]
ReC$_8$Re	198	217	230	192-197 dec[c]
ReC$_{10}$Re	161	188	206	170-180 dec[d]
ReC$_{12}$Re	160	178	211	180-210 dec[d]
ReC$_{16}$Re	175	205	220	150-180 dec[d]
ReC$_{20}$Re	135	155	201	130-150 dec[d]

Figure 4. Summary of DSC and capillary thermolysis data for polyynediyl complexes (°C). See footnote 28 for definition of terms. Table footnotes: [a]Sealed; conventional melting point apparatus. [b]*SS*,-*RR* diastereomer. [c]Forms viscous liquid. [d]Decomposition without melting, as assayed by IR (see text).

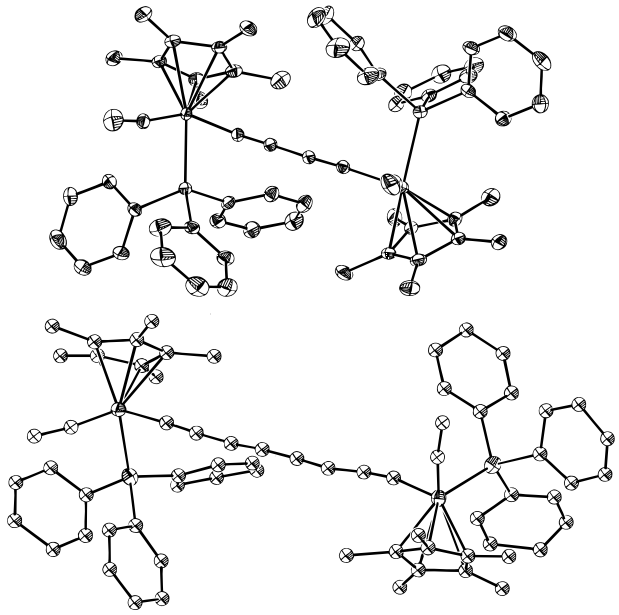

Figure 5. Molecular structures of the butadiynediyl and octatetraynediyl complexes **ReC$_4$R**e and **ReC$_8$Re**.

3. C$_{20}$ and C$_{24}$ Complexes. We sought to extend the methodology in Scheme 4 to still higher homologues. Thus, precursors with longer C_xH chains were required, and "second-generation" chain extensions were attempted. As shown in Scheme 6, reactions of **ReC$_6$H** and **ReC$_8$H** with *n*-BuLi and CuI similar to those above gave alkynyl copper species of empirical formulas **ReC$_6$Cu** and **ReC$_8$Cu**. The former could be isolated[33b,c] but was normally treated in situ with $EtNH_2$ and

Scheme 4. Syntheses of Hexatriynyl and Octatetraynyl Building Blocks

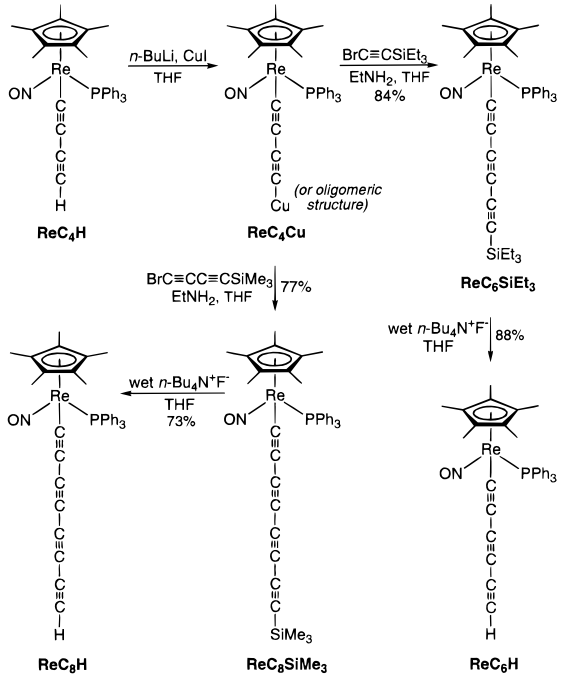

Scheme 5. Syntheses of Dodecahexaynediyl (C_{12}) and Hexadecaoctaynediyl (C_{16}) Complexes

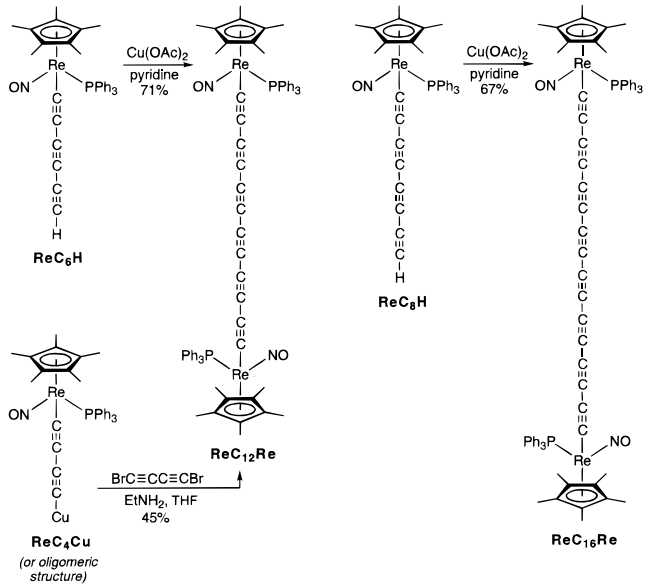

$BrC{\equiv}CC{\equiv}CSiMe_3$ as described for **ReC_4Cu**. Workup gave the analytically pure decapentaynyl complex **$ReC_{10}SiMe_3$** in 51% yield. Similar reactions of **ReC_6Cu** and $BrC{\equiv}CC{\equiv}CSiEt_3$[38] or **$ReC_8Cu$** and $BrC{\equiv}CSiEt_3$, gave the triethylsilyl analogue **$ReC_{10}SiEt_3$** in 44−26% yields.[35] An analogous coupling of **ReC_8Cu** and $BrC{\equiv}CC{\equiv}CSiMe_3$ gave the dodecahexaynyl complex **$ReC_{12}SiMe_3$** in 43% yield.

Reactions of **$ReC_{10}SiMe_3$** and K_2CO_3/MeOH or wet *n*-$Bu_4N^+F^-$/toluene (Scheme 6) gave **$ReC_{10}H$**, which was much more labile than the lower C_xH homologues and characterized only by IR, ^{31}P NMR, and mass spectroscopy. Crude **$ReC_{10}H$** was treated with $Cu(OAc)_2$ in pyridine at 50−60 °C. Workups gave the eicosadecaynediyl complex **$ReC_{20}Re$** as a black powder in

(38) Ghose, B. N.; Walton, D. R. M. *Synthesis* **1974**, *12*, 890.

Scheme 6. Synthesis of an Eicosadecaynediyl (C_{20}) Complex

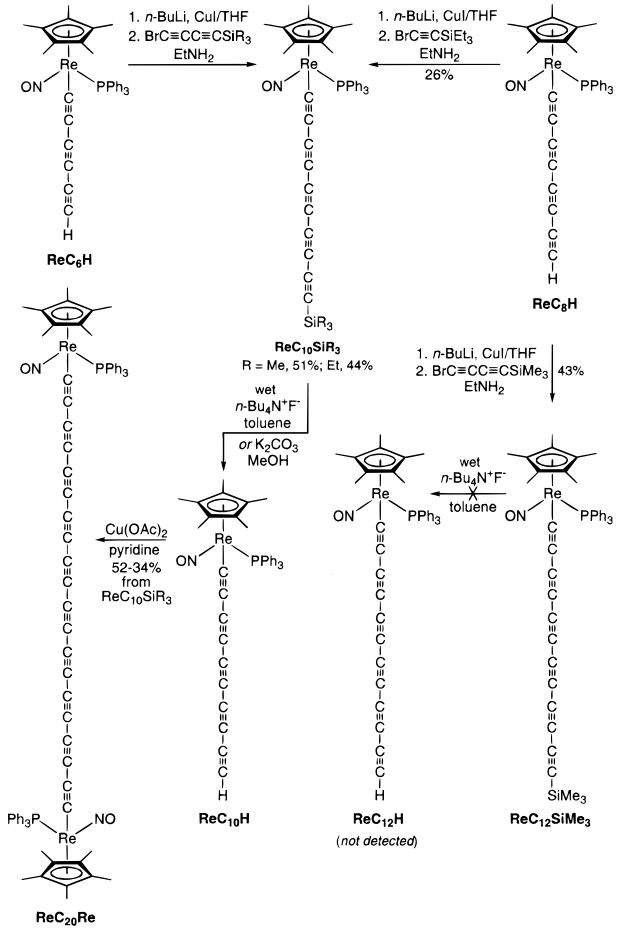

41−34% yields.[39] An analogous sequence with **$ReC_{10}SiEt_3$** and $Bu_4N^+F^-$ gave a slightly higher yield (52%). Samples were characterized identically to lower homologues. However, correct microanalyses could not be obtained. Figure 6 shows the ^{13}C NMR spectrum of **$ReC_{20}Re$**, together with that of **$ReC_{16}Re$**.

The stabilities of the title compounds merit careful description. Solid-state data are summarized in Figure 4. DSC gave a relatively high T_e or decomposition point[28] of 155 °C for **$ReC_{20}Re$**. The lower homologues exhibited still higher values (178−217 °C), but without any obvious trends. All were stable to air at room temperature on the time scale of hours. Samples were also slowly heated in sealed capillaries. Both **ReC_6Re** and **ReC_8Re** decomposed to viscous liquids. The other complexes decomposed gradually and without melting. To complement visual observations, several capillaries of a given sample were simultaneously heated. At various temperatures, one was removed, broken, and analyzed by IR (KBr).

In the case of **$ReC_{20}Re$**, the IR spectrum of material that had been heated to 130 °C showed no change. Material that had been heated to 140 °C showed a new, broad, medium-to-strong $\nu_{C\equiv C}$ band at 2101 cm^{-1}, and shifted bands at 2043 (medium to strong) and 1960 (s) cm^{-1} (slightly diminished relative to the ν_{NO} band). Little change occurred at 150 °C. Material that had been heated to 160 °C showed loss of resolution (but not intensity) in the $\nu_{C\equiv C}$ region. These data are consistent with, but do not by themselves establish, some type of chain−chain cross-linking process akin to the polymerization of 1,3-diynes.[40]

(39) The procedure that uses *n*-$Bu_4N^+F^-$ is given in the Supporting Information.

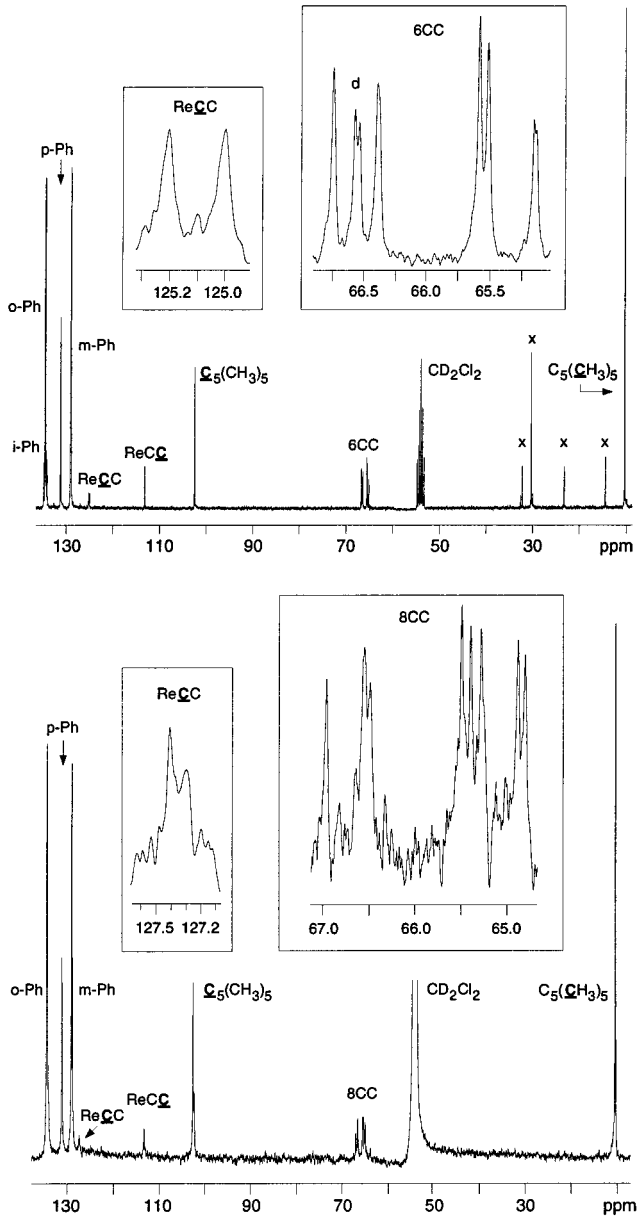

Figure 6. ^{13}C NMR spectra (CD_2Cl_2, 20 °C) of $\mathbf{ReC_{16}Re}$ (top, 75 MHz) and $\mathbf{ReC_{20}Re}$ (bottom, 126 MHz) and expanded insets; x = impurities in solvents, d = doublet.

Similar experiments with $\mathbf{ReC_{12}Re}$ showed little decomposition at 170 °C but a dramatic loss of signal intensity at 180 °C. At 190 °C, no residual $\nu_{C\equiv C}$ or ν_{NO} bands were apparent.

In solution, $\mathbf{ReC_{16}Re}$ and lower homologues exhibited normal stability properties and were not particularly air sensitive. However, $\mathbf{ReC_{20}Re}$ showed erratic behavior. For example, it could be recovered from some but not all spectroscopic measurements. For every NMR sample that unexpectedly decomposed, another would remain for several days under the most casual storage conditions. We were unable to reproducibly correlate this behavior to light, solvent, O_2 levels, or purity.

Reactions of $\mathbf{ReC_{12}SiMe_3}$ and wet n-$Bu_4N^+F^-$ in toluene immediately gave black, sootlike precipitates. Polyynediyl species with hydrogen endgroups commonly show much greater decreases in stabilities with chain length.[41] Hence, this was presumed to reflect the rapid decomposition of $\mathbf{ReC_{12}H}$. Therefore, the tetracosadodecaynediyl complex $\mathbf{ReC_{24}Re}$, which would probably be considerably more stable, cannot be accessed by the methodology described in this paper.

Discussion

1. Chain Length Effects. The wirelike title compounds constitute a unique and heretofore unavailable series of organotransition metal complexes. The rhenium atoms in the longest member, $\mathbf{ReC_{20}Re}$, are linked by 2 Re−C, 10 C≡C, and 9 ≡C−C≡ bonds, or a total of 21 σ and 20 π bonds. A rhenium−rhenium distance of 28.7 Å can be estimated from existing data.[12,15,23] Although there is more and more precedent for such metal−metal separations in the rapidly evolving area of molecular nanostructures,[42] the title compounds remain unsurpassed by the simplicity of the connecting unit.

As noted in the Introduction, only a few comparable families of polyynediyl compounds, all with carbon or silicon endgroups, have been previously isolated. These provide important opportunities to define the effect of chain length upon molecular properties, which should asymptotically approach those of valence forms **II** or **IV** of the polymeric sp carbon allotrope carbyne (Scheme 1). In principle, any observable quantity can be plotted against $1/n$, where n is the number of alkyne units. Extrapolation to the y intercept ($1/n = 0$) gives the value for the corresponding $(C\equiv C)_\infty$ species. In colloquial usage, we find the term "triple bond effect" useful. This underscores the difference from cumulated systems such as valence form **III**.

Consider first the effect of chain length upon bond lengths. Two types of asymptotic structural limits are possible. Will the C≡C and ≡C−C≡ distances converge to one value, or approach two different values? The former (bond length equalization) implies a vanishing HOMO/LUMO energy gap.[43] The latter (bond length alternation) requires a persistent energy gap, or from a solid-state physics perspective a Peierls distortion.[43b] We lack structural data for the title compounds beyond that represented by Figure 5. However, theoretical studies of the parent system $H(C\equiv C)_nH$ predict *two* limiting values (1.1956−1.2031 and 1.3574−1.3726 Å).[44] The longest polyynes structurally characterized to date, the diplatinum and diron dodecahexaynediyl complexes **Va**,**b** in Figure 7, show triple and single bonds in the ranges 1.210(5)−1.233(4)/1.19(1)−1.23(1) (**a**/**b**) and 1.344(7)−1.356(4)/1.35(1)−1.38(1) Å.[21b,23] Bond length alternation would also be expected by analogy to extensive data on polyenes and polyacetylene, $(CH{=}CH)_n$.[45] Additional aspects of this issue have been elegantly analyzed by Hirsch et al.[10]

Before a discussion of the spectroscopic properties of the title compounds, key features of monometallic or purely organic analogues merit a brief summary. First, alkynyl ligands are commonly poor π acceptors.[46] In 18-valence-electron complexes, repulsive interactions between occupied metal-based orbitals and ligand π orbitals dominate. The first few HOMOs are metal centered, with considerable d_{xy}, d_{xz}, and d_{yz} character

(40) For a reference list, see: Foley, J. L.; Li, L.; Sandman, D. J. *Chem. Mater.* **1998**, *10*, 3984.

(41) Yamaguchi, M.; Park, H.-J.; Hirama, M.; Torisu, K.; Nakamura, S.; Minami, T.; Nishihara, H.; Hiraoka, T. *Bull. Chem. Soc. Jpn.* **1994**, *67*, 1717.

(42) (a) The July 1999 issue of *Chemical Reviews* is devoted to this subject. (b) For nanostructures based upon simple axial rods, see: Schwab, P. F. H.; Levin, M. D.; Michl, J. *Chem. Rev.* **1999**, *99*, 1863.

(43) (a) Hoffmann, R. *Angew. Chem.* **1987**, *99*, 871; *Angew. Chem., Int. Ed. Engl.* **1987**, *26*, 846. (b) Rice, M. J.; Bishop, A. R.; Campbell, D. K. *Phys. Rev. Lett.* **1983**, *51*, 2136.

(44) Toto, J. L.; Toto, T. T.; de Melo, C. P.; Kirtman, B.; Robins, K. *J. Chem. Phys.*, **1996**, *104*, 8586 (see Table 1).

(45) Curran, S.; Stark-Hauser, A.; Roth, S. In *Handbook of Organic Conductive Molecules and Polymers*; Nalwa, H. S., Ed.; Wiley: 1997; Vol. 2, Chapter 1.

(46) Manna, J.; John, K. D.; Hopkins, M. D. *Adv. Organomet. Chem.* **1995**, *38*, 79.

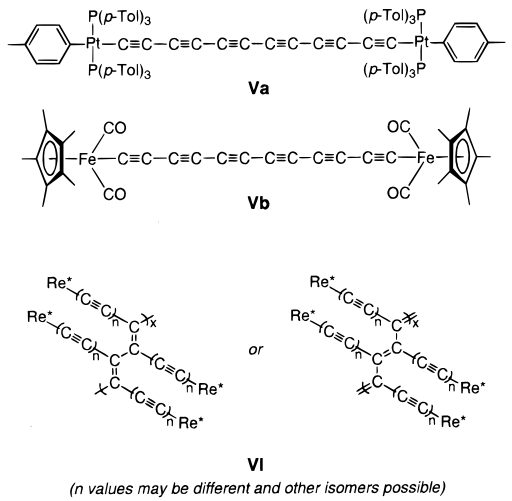

Figure 7. Other relevant structures.

in octahedral geometries. This bonding model is supported by numerous computational studies[12,17b,47] as well as photoelectron spectroscopy.[48,49] Photoelectron spectra of conjugated polyynes have also been recorded[50] and exhibit π MO energy patterns in accord with simple Hückel theory. Polyynes also have a σ inductive electron-withdrawing effect, which acidity measurements show to increase with chain length.[51]

2. IR, Raman, and NMR Spectra. Chiral rhenium complexes $[\mathbf{ReL}]^{n+}$ exhibit an intense IR ν_{NO} band that shifts according to both the amount of back-bonding from and the charge on rhenium, and hence the nature of the ancillary ligand L. Data for monorhenium complexes $\mathbf{ReC}_x\mathbf{SiR_3}$ and $\mathbf{ReC}_x\mathbf{H}$ are tabulated in the Supporting Information. Although the media employed vary, values increase from 1627 to 1637 cm^{-1} for $x = 2$ to an apparent limit of 1660−1662 cm^{-1} for $x = 10-12$. Thus, back-bonding to the nitrosyl ligand decreases. This trend is opposite to what might have been expected from the progressively higher π MO energies of the $(C{\equiv}C)_nSiR_3/H$ fragments, which through repulsive interactions can raise the energy of one d orbital used for nitrosyl ligand back-bonding. It is consistent with a progressively greater σ electron-withdrawing effect, which would generally lower the rhenium basicity.[52]

IR data for the dirhenium complexes $\mathbf{ReC}_x\mathbf{Re}$ are summarized in Table 1. In each case, measurements have been made in THF. The ν_{NO} values similarly increase from 1630 cm^{-1} for $x = 4$ to a clear limit of 1653−1654 cm^{-1} for $x = 12-20$, consistent with a dominant inductive effect. However, they remain lower than those of monorhenium complexes of identical chain length. This might reflect somewhat higher $(C{\equiv}C)_n$ π MO energy levels due to repulsive interactions with occupied rhenium d orbitals at each terminus. This opposing secondary effect would slightly increase back-bonding to the nitrosyl ligands, as analyzed above.

The IR $\nu_{C\equiv C}$ regions are richly featured. The monorhenium complexes generally show one band per alkyne unit, and representative spectra are provided in the Supporting Information. The extinction coefficients of the most intense bands increase with chain length, as gauged from ν_{NO} absorptions that should remain constant.[53] The dirhenium complexes exhibit approximately half the $\nu_{C\equiv C}$ bands of monorhenium complexes of equal chain length, consistent with their higher symmetry and IR selection rules. As expected, Raman spectra show complementary absorptions, especially at shorter chain lengths. Surprisingly, theoretical studies of vibrational spectra of polyynes appear to be scarce.[54]

Key ^{13}C NMR data for the monorhenium complexes are tabulated in the Supporting Information. The Re**C**≡ signals show steady downfield shifts with longer chain lengths (in ppm: $\mathbf{ReC_4SiMe_3/H}$, 102.1−105.8; $\mathbf{ReC_6SiMe_3/SiEt_3/H}$, 112.3−113.6; $\mathbf{ReC_8SiMe_3/H}$, 117.2−117.6; $\mathbf{ReC_{10}SiMe_3/SiEt_3}$, 122.7−122.9; $\mathbf{ReC_{12}SiMe_3}$, 125.2). Limiting values of 133−138 ppm for $\mathbf{ReC_\infty X}$ can be obtained graphically. At the opposite terminus, the C≡**C**Si signals show a similar but less pronounced approach to a 88−90 ppm limit. In contrast, the ReC≡**C** signals vary only slightly (110.8−113.4 ppm). The $^2J_{CP}$ values of chiral organorhenium complexes $[\mathbf{ReC}_x\mathbf{H}_y]^{n+}$ are sensitive to the rhenium−carbon bond order.[13c] However, they remain constant within experimental error (15.1−16.4 Hz), suggesting no significant increase of alkylidene character with chain length. Additional coupling features ($^2J_{CP} > {}^4J_{CP} > {}^3J_{CP}$) have been analyzed earlier.[13a]

Similar chemical shift and coupling constant patterns are evident for the dirhenium complexes $\mathbf{ReC}_x\mathbf{Re}$ in Table 2 and Figure 6. The Re**C**≡ signals show a broader range of $^2J_{CP}$ values (but a narrow 15.7−14.6 Hz spread for $x > 8$) and extrapolate to 133 ppm for $\mathbf{ReC_\infty Re}$. Another important feature becomes especially evident when the carbon chains terminate in identical endgroups. As illustrated in Figure 6, the interior ReC≡C(**C**≡**C**)$_n$C≡CRe signals cluster in the narrow range of 64−67 ppm. This can be taken as the chemical shift of carbyne in valence forms **II** and **IV** (Scheme 1). Identical limiting values are found for the series of dicyanides $NC(C{\equiv}C)_nCN$ purified by Hirsch et al.[10] and the mixtures characterized by Lagow et al.[6]

3. UV−Visible Spectra. Solutions of the title compounds deepen in color from orange ($\mathbf{ReC_8Re}$) to red ($\mathbf{ReC_{12}Re}$) to black cherry ($\mathbf{ReC_{16}Re}$) to brown-black ($\mathbf{ReC_{20}Re}$). Accordingly, UV−visible spectra exhibit progressively red-shifted and more intense bands, as illustrated in Figure 1. The molar extinction coefficients of $\mathbf{ReC_{16}Re}$ and $\mathbf{ReC_{20}Re}$ reach nearly 150 000 and 200 000 M^{-1} cm^{-1}. The latter complex absorbs over the entire visible range, reflecting a multitude of electronic transitions. Monorhenium complexes with identical chain lengths show roughly comparable absorptions ($\mathbf{ReC_{12}Re/ReC_{12}SiMe_3}$, four longest wavelength bands: 422/414, 470/468, 512/508, 568/554 nm; 83 000/70 000, 37 000/13 000, 17 000/14 000, 3900/11 000 M^{-1} cm^{-1}).

In contrast, polyynediyls with *tert*-butyl, trialkylsilyl, or cyano endgroups exhibit much simpler spectra and are not as deeply

(47) Key papers published after the period reviewed in ref 46: (a) McGrady, J. E.; Lovell, T.; Stranger, R.; Humphrey, M. G. *Organometallics* **1997**, *16*, 4004. (b) Belanzoni, P.; Re, N.; Sgamellotti, A.; Floriani, C. *J. Chem. Soc., Dalton Trans.* **1998**, 1825.

(48) Lichtenberger, D. L.; Renshaw, S. K.; Wong, A.; Tagge, C. D. *Organometallics* **1993**, *12*, 3522 and references therein.

(49) Photophysical studies of other octahedral rhenium alkynyl or butadiynediyl complexes are also consistent with these generalizations: (a) Yam, V. W.-W.; Lau, V. C.-Y.; Cheung, K.-K. *Organometallics* **1996**, *15*, 1740. (b) Yam, V. W.-W.; Cong, S. H.-F.; Cheung, K.-K. *J. Chem. Soc., Chem. Commun.* **1998**, 2121 and references therein.

(50) Gleiter, R.; Schäfer, W. In *The Chemistry of Triple-Bonded Functional Groups*; Patai, S., Ed.; John Wiley & Sons: Chichester, 1994; p 153.

(51) Eastmond, R.; Johnson, T. R.; Walton, D. R. M. *J. Organomet. Chem.* **1973**, *50*, 87.

(52) Of course, the $(C{\equiv}C)_nSiR_3/H$ fragments will exhibit progressively lower π^* MO energies. This can decrease the energy of one d orbital used for nitrosyl ligand back-bonding. However, we presently view this as a secondary influence in view of the studies cited above and other data below.

(53) For quantitative extinction coefficient measurements of related aldehyde complexes, see: Quirós Méndez, N.; Seyler, J. W.; Arif, A. M.; Gladysz, J. A. *J. Am. Chem. Soc.* **1993**, *115*, 2323.

(54) (a) Dudev, T.; Galabov, B. *Spectrochim. Acta, Part A* **1997**, *53*, 2053. (b) For a detailed IR and Raman study of polymers with $[-Pt(PR_3)_2(C{\equiv}C)-]_n$ ($n = 2, 3$) repeat units, see: Markwell, R. D.; Butler, I. S.; Kakkar, A. K.; Khan, M. S.; Al-Zakwani, Z. H.; Lewis, J. *Organometallics* **1996**, *15*, 2331.

colored. For example, $Et_3Si(C{\equiv}C)_8SiEt_3$ is isolated as white crystals[8] and $Me_3C(C{\equiv}C)_{10}CMe_3$ as orange or salmon needles.[7a] The latter represents the longest chain for which quantitative extinction coefficients are available. The longest wavelength band (320 nm) is the most intense, and the next longest wavelength band (303 nm) is the next most intense (ϵ 345 000 and 140 000 M^{-1} cm^{-1}, hexane). Similar values are reported for $Et_3Si(C{\equiv}C)_8SiEt_3$ (ϵ 447 000/331 000 and 398 000/295 000 M^{-1} cm^{-1} (hexane/methanol), 336/335 and 316/315 nm).[8] Analogous intensity patterns are exhibited by all of these compounds,[7a,10] including matrix-isolated $H(C{\equiv}C)_nH$ species.[55]

Despite the complexity of Figure 1, it is possible to suggest some assignments. The longest wavelength bands in polyynediyls with carbon, silicon, or hydrogen endgroups can confidently be attributed to $\pi \rightarrow \pi^*$ transitions. These are symmetry allowed, in accord with the high extinction coefficients. As described most recently by Hirsch et al., plots of energies versus $1/n$ are linear.[10] Importantly, these give values of approximately 550 nm for the analogous bands at infinite chain length, *irrespective of endgroup*. This corresponds to the limiting HOMO/LUMO energy gap for each series of compounds. Since they are essentially equal, a similar value can confidently be assigned to valence forms **II** and **IV** of carbyne.

As shown by Figure 1, the longest wavelength bands of **ReC$_x$Re** are never the most intense. Per the HOMO analysis above, these transitions would be expected to originate from orbitals with high rhenium d character. A possible analogy would be the $n \rightarrow \pi^*$ absorptions of ketones, which are symmetry forbidden and show much lower extinction coefficients. Regardless, we hypothesized that the most intense band in every spectrum represented the transition from the orbital with the greatest degree of $(C{\equiv}C)_n$ π HOMO character. The energies were plotted versus $1/n$, using maxima obtained from Gaussian curve fitting (Experimental Section). As depicted in the inset in Figure 1, a good linear correlation was found, giving 565 nm for the corresponding absorption in **ReC$_\infty$Re**.

In view of the agreement of this value with those of carbon-, silicon-, and hydrogen-capped polyynediyls, we provisionally assign the corresponding transitions as those with the highest degree of $\pi \rightarrow \pi^*$ character. However, we caution that the slope differs greatly from those of other plots.[10] An endgroup effect is to be expected, but it will be important to assay other $L_mM(C{\equiv}C)_nML_m$ systems. An analogous plot involving the best-defined longest wavelength bands of **ReC$_{12}$Re**, **ReC$_{16}$Re**, and **ReC$_{20}$Re** (472, 548, 610 nm after curve fitting) gives a value of 1082 nm for **ReC$_\infty$Re**. This might correspond to the limiting energy of an $n \rightarrow \pi^*$ type transition. Other polyynediyls with endgroups that bear lone pairs, such as $R_2N(C{\equiv}C)_nNR_2$, would constitute useful test compounds. However, none are yet available.

4. Redox Properties. The title compounds are unique among $C_{12}-C_{20}$ polyynediyl families in having redox-active endgroups. The cyclic voltammogram of **ReC$_4$Re** in Figure 2 shows two successive reversible one-electron oxidations corresponding to the radical cation **ReC$_4$Re**$^+PF_6^-$ and dication **ReC$_4$Re**$^{2+}2(PF_6^-)$ isolated in Scheme 2.[12] The other voltammograms illustrate the progressive decrease in reversibility with chain length. Reversibility is also lower in CH_3CN than in CH_2Cl_2. No reductions are observed prior to solvent-imposed limits. Data are summarized in Figure 3, and several trends are evident.

First, as the chain lengthens, the first oxidation potentials become thermodynamically less favorable (**ReC$_4$Re** vs **ReC$_{16}$Re**, $\Delta E^\circ = 0.56$ V). The second oxidation potentials are less strongly affected (**ReC$_4$Re**/**ReC$_6$Re** vs **ReC$_{16}$Re**, $\Delta E^\circ = 0.12/0.18$ V). Consequently, the E° values approach each other. With **ReC$_{20}$Re**, only a single—presumably two-electron—oxidation is observed. This signifies the chain length at which the two rheniums start to behave independently, at least in a redox sense. For statistical reasons, a small 0.036 V gap should persist.[56] However, this difference is often not resolved.[56b]

The trend in first oxidation potentials can be analyzed from several perspectives. First, in accord with other data above, it is inconsistent with HOMOs that have dominant $(C{\equiv}C)_n$ π character. Otherwise, oxidation would be thermodynamically more favorable at longer chain lengths. Second, inductive effects can contribute. For example, **ReC$_4$Me** is 0.08 V more difficult to oxidize than **ReC$_2$Me**.[13a] Third, resonance effects are also possible. As analyzed in a previous full paper,[12] **ReC$_4$Re**$^+PF_6^-$ is a class III mixed-valence system,[57] with the odd electron completely delocalized between the two rheniums on the rapid IR and ESR time scales. By analogy to other systems in the literature,[56b,57] the electronic coupling or resonance energy should decrease with bridge length. Hence, this additional thermodynamic driving force will be greatest for **ReC$_4$Re**.

The second oxidation potentials fall into a narrower range. Except for **ReC$_4$Re**$^+X^-$, they also shift monotonically in a thermodynamically less favorable direction. The unique position of **ReC$_4$Re**$^+X^-$ compared to those of the three next higher homologues might be due to an extraordinarily high resonance energy, or Coulombic repulsion associated with introducing the second positive charge. The second and first oxidation potentials yield comproportionation constants (K_c, Figure 3), which are defined as exemplified in Scheme 2. These generally track other measures of electronic communication between the endgroups[12,16,57] and, as expected, decrease with chain length.

Despite the quite reversible electrochemical generation of the C_6 and C_8 radical cations and dications, attempts at preparative oxidations have been disappointing. Substituted ferrocenium salts give rapid oxidations at -80 °C, and IR ν_{NO} bands consistent with radical cations (as well as other new ν_{NO} bands) can be detected. However, the primary products are unstable at low temperatures. Similar experiments with 2 equiv of ferrocenium salts give some NMR signals consistent with dications, but rapid decompositions again ensue. Figure 5 shows that the carbon chains become much more "exposed", and thus susceptible to intermolecular reactions, with increasing length. One possibility for the radical cations would be carbon—carbon bond-forming dimerizations analogous to those of some 17-valence-electron alkynyl complexes.[16a,58]

Accordingly, we have designed modified rhenium endgroups that provide radical cations and dications with higher thermodynamic and kinetic stabilities. The isolation of C_8 species will be reported soon.[29b] These modified systems exhibit much more reversible couples, which will allow better interpretation of the trends in Figure 3 and other important properties. For example, there should be a chain length at which radical cations are no longer delocalized on the IR time scale, and perhaps another at which they are no longer delocalized on the slightly slower ESR

(55) See Figures 1 and 4 in the following paper: Grutter, M.; Wyss, M.; Fulara, J.; Maier, J. P. *J. Phys. Chem. A* **1998**, *102*, 9785 (**HC$_{12}$H** through **HC$_{24}$H**).

(56) (a) Flanagan, J. B.; Margel, S.; Bard, A. J.; Anson, F. C. *J. Am. Chem. Soc.* **1978**, *100*, 4248. (b) McWhinnie, S. L. W.; Thomas, J. A.; Hamor, T. A.; Jones, C. J.; McCleverty, J. A.; Collison, D.; Mabbs, F. E.; Harding, C. J.; Yellowlees, L. J.; Hutchings, M. G. *Inorg. Chem.* **1996**, *35*, 760.

(57) (a) Creutz, C. *Prog. Inorg. Chem.* **1983**, *30*, 1. (b) Crutchly, R. J. *Adv. Inorg. Chem.* **1994**, *41*, 273.

(58) (a) Iyer, R. S.; Selegue, J. P. *J. Am. Chem. Soc.* **1987**, *109*, 910. (b) Unseld, D.; Krivykh, V. V.; Heinze, K.; Wild, F.; Artus, G.; Schmalle, H.; Berke, H. *Organometallics* **1999**, *18*, 1525.

time scale. In the same vein, Lapinte et al. have found a diiron C_4 dication with closely lying $S = 0$ (cumulenic) and $S = 1$ (biradical) states.[16a,c] Such equilibria should also be highly chain-length-dependent.

5. Syntheses and Stabilities. The key factors controlling the pace of future progress in this field are synthetic methods and product stabilities. The reaction types employed above have been discussed in previous full papers or notes,[12,15] so strategic issues are emphasized here. First, the number of steps required to access **ReC$_{20}$Re**, and the yield drop-off with the "second-generation" chain extensions in Scheme 6, clearly point to the desirability of longer sp carbon building blocks. Earlier, we reported an efficient route to $Me_3SiC{\equiv}CC{\equiv}CC{\equiv}CC{\equiv}CSiMe_3$.[13a] However, we have been unable to develop methods that utilize this material directly or efficiently desymmetrize it to a monohaloalkyne that could undergo Cadiot−Chodkiewicz coupling. We are not aware of other useful C_8 building blocks that meet reasonable standards of accessibility or safety.

Convergence is also highly desirable in syntheses, especially for symmetrical molecules. One route to **ReC$_{12}$Re** makes use of three C_4 building blocks: **ReC$_4$Cu**, $BrC{\equiv}CC{\equiv}CBr$, and **ReC$_4$Cu** (Scheme 5). However, attempted extensions involving **ReC$_6$Cu** and $BrC{\equiv}CC{\equiv}CBr$ or $BrC{\equiv}CC{\equiv}CC{\equiv}CC{\equiv}CBr$[37] were unsuccessful. Also, $XC{\equiv}CX$ coupling partners would lead to systems with odd numbers of alkyne units, which are otherwise available only as mixtures (**ReC$_6$Re**, Scheme 3; **ReC$_{10}$Re**). As noted above, all cases investigated gave at best traces of the target complex. Regardless, the procedures given for mono- and dihaloalkynes in this paper and previous ones[15] are highly optimized and should be of utility to others.

As summarized in Figure 4, the title compounds exhibit remarkable stability in the solid state. Over years of study, no explosions have occurred. With respect to synthesis, these favorable characteristics suggest that **ReC$_{24}$Re** should, in principle, be accessible. However, we are presently blocked by the instability of **ReC$_{12}$H**, which is not detectable under the standard deprotection conditions in Scheme 6. Thus, oxidative couplings that avoid hydrogen-capped chains should prove valuable in future work. One literature protocol did convert **ReC$_4$SiMe$_3$** directly to **ReC$_8$Re**,[59] but it was judged unpromising due to the slow rate, workup problems due to excess oxidant, and the likely intermediacy of **ReC$_4$H**. Interestingly, reactions of **ReC$_x$H** and $Cu(OAc)_2$ become more rapid at higher chain lengths, despite an opposite trend in oxidation potentials.

On the basis of the limited IR $\nu_{C\equiv C}$ and ν_{NO} data above, we propose that the thermal decompositions in Figure 4 involve initial chain−chain cross-linking. This has abundant precedent with a broad spectrum of 1,3-diynes.[40] The resulting oligomers or polymers would feature an extended unsaturated network of C═C and C≡C units, some possible motifs for which are shown in Figure 7 (**VI**). Such materials also constitute attractive targets for future research. They are related to polyacetylene and might similarly give conducting materials when doped.[45] The lability of **ReC$_{20}$Re** in solution might reflect an analogous impurity-catalyzed cross-linking or an entirely different decomposition mechanism.

The kinetic stabilities of polyynediyls are known to be strong functions of the endgroups.[8−10] Hydrogen obviously offers unique decomposition pathways. Smaller groups such as methyl are believed to facilitate chain−chain reactions. At present, there is no quantitative way to compare the stabilities of **ReC$_x$Re** with those of related *tert*-butyl, trialkylsilyl, or cyano systems. However, we suggest that bulky electropositive endgroups, which complement the somewhat electronegative sp carbon terminus, will generally be good choices. Thus, transition metals are likely to play leading roles in the future development of this field.

6. Conclusion and Outlook. Rational syntheses of rhenium-capped polyynediyls that are as long as 20 carbons have been developed. These wirelike systems provide valuable models for valence forms **II** and **IV** of the polymeric sp carbon allotrope carbyne (Scheme 1). Their spectroscopic, stability, and redox properties have been rigorously characterized as a function of chain length. Ongoing work involves analogues with modified phosphines that afford radical cations and dications with much greater stabilities. The latter provide new models for valence form **III** of carbyne. These second-generation complexes allow a variety of properties to be even more precisely defined.

Experimental Section[60,61]

ReC$_8$Re. A Schlenk flask was charged with **ReC$_4$H** (0.066 g, 0.10 mmol),[13a] $Cu(OAc)_2$ (0.027 g, 0.15 mmol), and pyridine (3 mL). The mixture was stirred at 80 °C for 2 h. Solvent was removed by oil pump vacuum. The residue was dissolved in THF (ca. 2 mL). Silica gel column chromatography (15 × 2 cm; THF) gave an orange-red band. Solvent was removed by oil pump vacuum to give **ReC$_8$Re** as an orange powder (0.047 g, 0.036 mmol, 70%).[62,63] Anal. Calcd for $C_{64}H_{60}N_2O_2P_2Re_2$: C, 58.08; H, 4.57. Found: C, 58.08; H, 4.98. R_f[64] = 0.50. UV−vis (3.3×10^{-5} M):[65] 234 (58 000), 262 sh (36 000), 340 sh (56 000), 360/*360* (67 000), 390/*390* (60 000). MS:[66a] 1324 (**ReC$_8$Re**$^+$, 100%), 614 (**Re**$^+$, 37%); no other peaks above 310 of >13%.

NMR:[67] ^{1}H (THF-d_8) 7.60−7.54 (m, 12H of $6C_6H_5$), 7.40−7.36 (m, 18H of $6C_6H_5$), 1.73 (s, $2C_5(CH_3)_5$); $^{13}C\{^1H\}$ (CD_2Cl_2/THF-d_8) 134.9/135.8 (d, J_{CP} = 52.9/51.6, *i*-Ph), 134.4/134.9 (d, J_{CP} = 9.6/10.4, *o*-Ph), 130.8/130.9 (s, *p*-Ph), 128.8/128.9 (d, J_{CP} = 9.3/9.6, *m*-Ph), 112.7/113.3 (s, ReC*C*), 111.0/109.7 (d, J_{CP} = 18.4/16.9, ReC), 101.7/101.5 (s, $\underline{C}_5(CH_3)_5$), 66.8/66.6 (d, J_{CP} = 2.9/2.7, ReC*C*C), 63.8/64.5 (s, ReC*C*C*C*), 10.3/10.1 (s, $C_5(\underline{C}H_3)_5$); $^{31}P\{^1H\}$ (THF-d_8) (ambient temperature/−80 °C) 20.7/20.8 (s).

ReC$_6$Re. A Schlenk flask was charged with **ReC$_2$H** (0.100 g, 0.157 mmol),[25] **ReC$_4$H** (0.104 g, 0.157 mmol), $Cu(OAc)_2$ (0.085 g, 0.47 mmol), and pyridine (5 mL). The mixture was stirred at 80 °C for 2 h. Solvent was removed by oil pump vacuum. The residue was dissolved in THF (ca. 3 mL). Silica gel column chromatography (8 × 2 cm; THF) gave an orange-red band. Solvent was removed by oil pump vacuum. A second silica gel column (20 × 2 cm; 3:1 v/v hexane/THF)

(59) Haley, M. M.; Bell, M. L.; Brand, S. C.; Kimball, D. B.; Pak, J. J.; Wan, W. B. *Tetrahedron Lett.* **1997**, *38*, 7483.

(60) General procedures, solvent and reagent purifications, and instrumental methods are described in the Supporting Information. **Re** = (η^5-C_5Me_5)Re(NO)(PPh_3).

(61) The compounds in this paper have distinctive IR $\nu_{C\equiv C}$ fingerprints that facilitate reaction monitoring. This footnote is used to highlight steps where IR monitoring is especially recommended.

(62) DSC data for this material are given in Figure 4.

(63) IR data for this material are given in Table 1.

(64) TLC plates, Merck, DC-Fertigplatten, Kieselgel 60 F_{254}, 1:1 v/v hexanes/THF.

(65) All UV−visible spectra were recorded in CH_2Cl_2. Absorbances are in nm (ϵ, M^{-1} cm^{-1}). Italicized values were obtained by Gaussian curve fitting of digitized spectra (PeakFit 4.0, Jandel Scientific; autofit peaks III deconvolution option with amplitude threshold 3%, width 5.0, and filter 75). These maxima were used in all graphical analyses (Figure 1, inset).

(66) Positive FAB, 3-NBA, *m/z*, are for the most intense peak of isotope envelope; relative intensities are for the specified mass range. (a) Benzene; (b) toluene; (c) THF; (d) $CHCl_3$; (e) CH_2Cl_2.

(67) The ^{1}H, ^{13}C, and ^{31}P NMR chemical shifts are in δ, ppm, and ppm, respectively, and J values are in Hz. Data relevant to ≡C ^{13}C NMR assignments are as follows: (a) Earlier work[13a] with butadiynyl complexes **ReC$_4$X** established the trend $^2J_{CP} > {}^4J_{CP} > {}^3J_{CP}/{}^5J_{CP}$. The last two have not yet proved detectable. Therefore, any broadened signal is provisionally assigned to ReC≡CC≡C*C* ($^6J_{CP}$). (b) The Re*C*≡*C* signals are normally farthest downfield. (c) Any ≡CH signal is the most intense. (d) The *C*≡*C*Si signals are normally downfield of internal *C*≡*C* signals, which are the most shielded due to well-established anisotropy effects. (e) A useful table of ^{13}C NMR data for various $L_mM(C{\equiv}C)_nX$ species has been compiled.[21a]

gave three orange bands, which were collected separately. Solvents were removed by oil pump vacuum to give **ReC$_4$Re** (0.028 g, 0.022 mmol, 14%), **ReC$_6$Re** (0.088 g, 0.068 mmol, 44%), and **ReC$_8$Re** (0.030 g, 0.023 mmol, 15%) as orange powders. Data for **ReC$_6$Re**:[62,63] Anal. Calcd for $C_{62}H_{60}N_2O_2P_2Re_2$: C, 57.30; H, 4.64. Found: C, 57.25; H, 4.78. R_f[64] = 0.51. UV−vis (1.6×10^{-5} M):[65] 232 (62 000), 328/*326* (39 000), 354/*352* (37 000). MS:[66a] 1300 (**ReC$_6$Re$^+$**, 100%), 614 (**Re$^+$**, 62%); no other peaks above 330 of >18%.

NMR:[67] ^{1}H (THF-d_8) 7.64−7.58 (m, 12H of 6C$_6$H$_5$), 7.40−7.35 (m, 18H of 6C$_6$H$_5$), 1.72 (s, 2C$_5$(CH$_3$)$_5$); ^{13}C{^{1}H} (CD_2Cl_2/THF-d_8, −80 °C) 135.3/136.3 (d, J_{CP} = 52.7/49.2, *i*-Ph), 134.5/135.1 (d, J_{CP} = 10.7/10.5, *o*-Ph), 130.6/130.7 (d/s, J_{CP} = 2.2/-, *p*-Ph), 128.7/128.8 (d, J_{CP} = 10.7/10.0, *m*-Ph), 112.6/114.3 + 113.9 (s/2s, *RR*,*SS* + *RS*,*SR* ReC$\underline{C}$), 106.8 + 106.5/104.2 + 103.3 (2d/2d, J_{CP} = 16.8 + 16.0/15.7 + 16.0, *RR*,*SS* + *RS*,*SR* Re$\underline{C}\underline{C}$), 101.3/100.8 (s, $\underline{C}_5$(CH$_3$)$_5$), 65.0 + 64.9/65.7 + 65.2 (2br s/2br s, *RR*,*SS* + *RS*,*SR* ReC$\underline{C}\underline{C}$), 10.3/10.0 (s, C$_5$($\underline{C}H_3$)$_5$); ^{31}P{^{1}H} (THF-$d_8$, ambient temperature/−80 °C) 21.2/21.1 (s).

ReC$_6$SiEt$_3$,[15b] ReC$_8$SiMe$_3$,[15a] and ReC$_6$H.[15b] These syntheses were published in connection with other studies, and optimized procedures are given in the Supporting Information.

ReC$_8$H. Procedure A. A Schlenk flask was charged with **ReC$_8$SiMe$_3$** (0.0455 g, 0.0581 mmol), freshly ground K_2CO_3 (0.0081 g, 0.058 mmol), and MeOH (5 mL). The mixture was stirred vigorously. After 24 h, solvent was removed by oil pump vacuum. The residue was extracted with toluene (2 × 3 mL). The extract was filtered through a 1-cm Celite pad, concentrated by oil pump vacuum (ca. 1 mL), diluted with hexane (10 mL), and kept at −40 °C (freezer) for 16 h. A red-brown powder was collected by filtration and dried by oil pump vacuum to give **ReC$_8$H** (0.0297 g, 0.0418 mmol, 72%), mp 128 °C dec. Anal. Calcd for $C_{36}H_{31}NOPRe$: C, 60.86; H, 4.39. Found: C, 60.21; H, 4.50. IR (cm^{-1}, THF/KBr): $\nu_{C\equiv C}$ 2109/2101 s, 2036/2031 s/m, 1971/1969 m/s, ν_{NO} 1659/1656 vs. UV−vis (2.8×10^{-6} M):[65] 232 (54 000), 262 sh (35 000), 312 sh (31 000), 336 sh (64 000), 378 (11 000), 418 (6300), 450 (4100). MS:[66b] 711 (**ReC$_8$H$^+$**, 100%), 614 (**Re$^+$**, 25%); no other peaks above 560 of >25%.

Procedure B. A Schlenk flask was charged with **ReC$_8$SiMe$_3$** (0.2810 g, 0.3588 mmol) and THF (10 mL). Then *n*-Bu$_4$N$^+$F$^-$ (1.0 M in THF/5 wt % H_2O; 0.089 mL, 0.089 mmol) was added dropwise with stirring. After 0.5 h, the mixture was filtered through a 1-cm silica gel pad. Solvent was removed from the filtrate by oil pump vacuum. The residue was dissolved in a minimum of benzene (ca. 3 mL), and hexane (50 mL) was added. The sample was kept at −20 °C (freezer) for 16 h. A dark red powder was isolated by filtration and dried by oil pump vacuum to give **ReC$_8$H** (0.1864 g, 0.2622 mmol, 73%).

NMR (C_6D_6):[67] ^{1}H 7.64−7.58 (m, 6H of 3C$_6$H$_5$), 7.06−6.95 (m, 9H of 3C$_6$H$_5$), 1.48 (s, C$_5$(CH$_3$)$_5$), 1.43 (d, J_{HP} = 1.0, ≡CH); ^{13}C{^{1}H} 135.3 (*i*-Ph),[68] 134.5 (d, J_{CP} = 10.7, *o*-Ph), 130.9 (s, *p*-Ph), 128.7 (d, J_{CP} = 10.0, *m*-Ph), 117.2 (d, J_{CP} = 15.8 Re$\underline{C}$C), 113.2 (s, ReC$\underline{C}$), 101.5 (s, $\underline{C}_5$(CH$_3$)$_5$), 70.2 (s, $\underline{C}$CH), 65.0, 64.1 (2 s, ReCCC$\underline{C}\underline{C}\underline{C}$), 68.2 (s, C$\underline{C}$H), 65.4 (d, J_{CP} = 2.8, ReCC$\underline{C}$), 64.5 (br s, ReCC$\underline{C}\underline{C}$C), 10.2 (s, C$_5$($\underline{C}H_3$)$_5$); ^{31}P{^{1}H} 20.4 (s).

ReC$_{10}$Re. A Schlenk tube was charged with **ReC$_4$SiMe$_3$** (0.161 g, 0.219 mmol),[13a] **ReC$_6$SiEt$_3$** (0.175 g, 0.219 mmol), and toluene (20 mL). Then *n*-Bu$_4$N$^+$F$^-$ (1.0 M in THF/5 wt % H_2O; 0.22 mL, 0.22 mmol) was added dropwise with stirring. After 0.5 h, the sample was cannulated into a 60 °C solution of Cu(OAc)$_2$ (0.119 g, 0.657 mmol) in pyridine (20 mL). After 0.5 h, solvent was removed by oil pump vacuum. The residue was extracted with THF (3 × 10 mL). The extract was filtered through a 7-cm silica gel pad. Solvent was removed by oil pump vacuum. Silica gel column chromatography (50 × 6 cm; 3:1 v/v hexane/ THF) gave three partially resolved bands. The center cut of the middle band contained **ReC$_{10}$Re** and minor amounts of **ReC$_8$Re** and **ReC$_{12}$Re**. A second identical column gave **ReC$_{10}$Re** as an orange powder (0.0261 g, 0.0194 mmol, 9%).[62,63] Anal. Calcd for $C_{66}H_{60}N_2O_2P_2Re_2$: C, 58.83; H, 4.49. Found: C, 58.58; H, 4.75. R_f[64] = 0.46. UV−vis (1.2×10^{-5} M):[65] 230 (58 000), 268 (32 000), 274 (32 000), 338 sh (41 000), 366 sh (59 000), 394/*394* (76 000), 426/*418* sh (50 000), 474/*470* sh (10 000). MS:[66c] 1348 (**ReC$_{10}$Re$^+$**, 100%), 614 (**Re$^+$**, 56%); no other peaks above 400 of >10%.

NMR (CD_2Cl_2):[67] ^{1}H 7.54−7.46 (m, 12H of 6C$_6$H$_5$), 7.45−7.39 (m, 18H of 6C$_6$H$_5$), 1.74 (s, 2C$_5$(C$\underline{H}_3$)$_5$); ^{13}C{^{1}H} 134.4 (d, J_{CP} = 10.7, *o*-Ph), 131.0 (s, *p*-Ph), 128.9 (d, J_{CP} = 10.1, *m*-Ph),[68] 117.3 (d, J_{CP} = 15.7, Re$\underline{C}$C), 112.7 (s, ReC$\underline{C}$), 101.9 (s, $\underline{C}_5$(CH$_3$)$_5$), 66.3, 64.1 (2 s, ReCCC$\underline{C}\underline{C}$), 66.1 (d, J_{CP} = 2.7, ReCC$\underline{C}$), 10.3 (s, C$_5$($\underline{C}$H$_3$)$_5$); ^{31}P{^{1}H} 19.9 (s).

ReC$_{12}$Re. Procedure A. A Schlenk flask was charged with **ReC$_6$H** (0.069 g, 0.10 mmol), Cu(OAc)$_2$ (0.018 g, 0.10 mmol), and pyridine (5 mL). The mixture was stirred at 50 °C for 0.5 h. Solvent was removed by oil pump vacuum. The residue was extracted with THF (2 × 5 mL). The extract was concentrated (ca. 2 mL). Silica gel column chromatography (20 × 2 cm; 2:1 → 1:2 v/v hexane/THF) gave an orange-red band, which was concentrated by oil pump vacuum (ca. 2 mL). Hexane (10 mL) was added. The orange-brown powder was collected by filtration and dried by oil pump vacuum to give **ReC$_{12}$Re** (0.048 g, 0.071 mmol, 71%).[62,63] Anal. Calcd for $C_{68}H_{60}N_2O_2P_2Re_2$: C, 59.11; H, 4.37. Found: C, 59.25; H, 4.65. R_f[64] = 0.43. UV−vis (1.4×10^{-5} M):[65] 230 (61 000), 280 (48 000), 364 sh (47 000), 390/*390* (63 000), 422/*422* (83 000), 470/*472* (37 000), 512 sh (17 000), 568 (3900). MS:[66a] 1372 (**ReC$_{12}$Re$^+$**, 100%), 614 (**Re$^+$**, 55%); no other peaks above 555 of >26%.

Procedure B. A Schlenk flask was charged with **ReC$_4$H** (0.066 g, 0.10 mmol) and THF (5 mL) and cooled to −45 °C (CO_2/CH_3CN). Then *n*-BuLi (2.2 M in hexane; 50 mL, 0.11 mmol) was added with stirring. After 2 h, the cold bath was removed, and CuI (0.019 g, 0.10 mmol) was added. After 30 min, the mixture was cooled to −20 °C, and $EtNH_2$ (ca. 0.5 mL) was added. A solution of BrC≡CC≡CBr (0.01 g, 0.05 mmol)[36] in THF (1 mL) was added dropwise. After 10 min, solvent was removed by oil pump vacuum. The residue was extracted with THF (2 × 5 mL), and chromatography as in procedure A gave **ReC$_{12}$Re** as an orange-brown powder (0.031 g, 0.022 mmol, 45%).

NMR:[67] ^{1}H (CD_2Cl_2/C_6D_6) 7.52−7.46/7.68−7.60 (m, 12H of 6C$_6$H$_5$), 7.46−7.42/7.05−6.94 (m, 18H of 6C$_6$H$_5$), 1.75/1.51, (s, 2C$_5$(CH$_3$)$_5$); ^{13}C{^{1}H} (CD_2Cl_2/C_6D_6)/135.0 (d, J_{CP} = 49.7, *i*-Ph),[68] 134.4/134.5 (d, J_{CP} = 10.4/10.7, *o*-Ph), 131.0/130.8 (s/d, J_{CP} = 2.0, *p*-Ph), 128.9/128.9 (d, J_{CP} = 10.1/10.1, *m*-Ph), 116.8/117.6 (d, J_{CP} = 15.6/15.7, Re$\underline{C}$C), 113.7/114.1 (s, ReC$\underline{C}$), 102.1/101.5 (s/d, J_{CP} = 1.2, $\underline{C}_5$(CH$_3$)$_5$), 67.1/67.4, 66.3/66.8, 64.4/66.0 (3 s, ReCCC$\underline{C}\underline{C}\underline{C}$), 66.0/66.5 (d, J_{CP} = 3.3/2.8, ReCC$\underline{C}$), 10.3/10.2 (s, C$_5$($\underline{C}$H$_3$)$_5$); ^{31}P{^{1}H} (C_6D_6) 22.2 (s).

ReC$_{16}$Re. A Schlenk flask was charged with **ReC$_8$H** (0.032 g, 0.045 mmol), Cu(OAc)$_2$ (0.008 g, 0.045 mmol), and pyridine (2.5 mL). The mixture was stirred at 50 °C for 0.5 h. Solvent was removed by oil pump vacuum. The residue was extracted with THF (2 × 2 mL). The extract was filtered through a 2-cm silica gel pad. Silica gel column chromatography (30 × 2 cm; 3:1 → 2:1 v/v hexane/THF) gave a dark red band. Solvent was removed by oil pump vacuum to give **ReC$_{16}$Re** as a dark red powder (0.043 g, 0.030 mmol, 67%).[62,63] Anal. Calcd for $C_{72}H_{60}N_2O_2P_2Re_2$: C, 60.91; H, 4.26. Found: C, 60.99; H, 4.32. R_f[64] = 0.39. UV−vis (2.1×10^{-5} M):[65] 232 (63 000), 328 (62 000), 348 (65 000), 402 sh (82 000), 430/*432* (140 000), 470/*470* (130 000), 548/*548* (61 000), 644 (9900). MS:[66d] 1420 (**ReC$_{16}$Re$^+$**, 50%), 614 (**Re$^+$**, 100%); no other peaks above 225 of >40%.

NMR:[67] ^{1}H (CD_2Cl_2) 7.55−7.46 (m, 12H of 6C$_6$H$_5$), 7.46−7.40 (m, 18H of 6C$_6$H$_5$), 1.66 (s, 2C$_5$(CH$_3$)$_5$); ^{13}C{^{1}H} (CD_2Cl_2) 134.4 (d, J_{CP} = 52.6, *i*-Ph), 134.4 (d, J_{CP} = 10.1, *o*-Ph), 131.2 (s, *p*-Ph), 129.0 (d, J_{CP} = 10.4, *m*-Ph), 125.1 (d, J_{CP} = 15.2, Re$\underline{C}$C), 113.2 (s, ReC$\underline{C}$), 102.5 (s, $\underline{C}_5$(CH$_3$)$_5$), 66.6 (d, J_{CP} = 2.4, ReCC$\underline{C}$), 66.7, 66.4, 65.6, 65.5, 65.2 (5 s, ReCCC$\underline{C}\underline{C}\underline{C}\underline{C}\underline{C}$), 10.3 (s, C$_5$($\underline{C}H_3$)$_5$); ^{31}P{^{1}H} ($C_6D_6$) 22.0 (s).

ReC$_{10}$SiMe$_3$. Procedure A. A Schlenk flask was charged with **ReC$_6$H** (0.069 g, 0.10 mmol), CuI (0.019 g, 0.10 mmol), and THF (5 mL) and cooled to −45 °C. Then *n*-BuLi (2.2 M in hexane; 50 mL, 0.11 mmol) was added with stirring.[61] The cold bath was removed. After 30 min, the mixture was cooled to −20 °C, and $EtNH_2$ (ca. 0.5 mL) was added. A solution of BrC≡CC≡CSiMe$_3$ (0.022 g, 0.11 mmol)[15a] in THF (2 mL) was added dropwise. After 10 min, solvent was removed by rotary evaporation. The residue was extracted with toluene (2 × 3 mL). The extract was filtered through a 2-cm silica gel

(68) The *i*-Ph resonance is not observed, or the upfield line of the doublet is obscured by the *o*-Ph or solvent resonance.

pad, and solvent was removed by oil pump vacuum. The residue was dissolved in a minimum of toluene (ca. 1 mL), and hexane was added (ca. 10 mL). The mixture was kept at −90 °C (freezer) for 24 h. Orange-brown microcrystals were isolated by filtration (−80 °C) and dried by oil pump vacuum to give **ReC$_{10}$SiMe$_3$** (0.041 g, 0.051 mmol, 51%), mp 160−165 °C dec. Anal. Calcd for $C_{41}H_{39}NOPReSi$: C, 60.65; H, 4.84. Found: C, 60.88; H, 4.97. R_f[64] = 0.61. IR (cm^{-1}, THF): $\nu_{C\equiv C}$ 2158 w, 2133 w, 2070 w, 2037 vs, 1955 vs, ν_{NO} 1662 s. UV−vis (1.7 × 10^{-5} M):[65] 270 (54 000), 280 (55 000), 296 (45 000), 330 (33 000), 356 (51 000), 382 (80 000), 434 (8900), 470 (10 000), 514 (8100). MS:[66e] 807 (**ReC$_{10}$SiMe$_3^+$**, 100%), 614 (**Re**$^+$, 25%); no other peaks above 100 of >15%.

For procedures B and C, see Supporting Information.

NMR (CD_2Cl_2):[67] ^{1}H 7.53−7.39 (m, 3C$_6$H$_5$), 1.75 (s, C$_5$(CH$_3$)$_5$), 0.20 (s, SiMe$_3$); ^{13}C{^{1}H} 134.3 (d, J_{CP} = 46.8, *i*-Ph), 134.3 (d, J_{CP} = 11.0, *o*-Ph), 131.1 (s, *p*-Ph), 128.9 (d, J_{CP} = 9.7, *m*-Ph), 122.9 (d, J_{CP} = 15.1, ReC$\underline{C}$), 112.7 (s, ReC$\underline{C}$), 102.2 (s, $\underline{C}_5$(CH$_3$)$_5$), 88.7, 88.6 (2 s, $\underline{CC}$Si), 65.7 (d, J_{CP} = 3.0, ReCC$\underline{C}$), 64.2 (d, J_{CP} = 1.8, ReCCCC$\underline{C}$, tentative), 65.5, 65.2, 63.7, 63.5 (4 s, ReCCC$\underline{C}$C$\underline{CCC}$), 10.2 (s, C$_5$-($\underline{C}$H$_3$)$_5$), 0.2 (s, SiCH$_3$); ^{31}P{^{1}H} 21.8 (s).

ReC$_{10}$SiEt$_3$. Procedure A. A Schlenk flask was charged with **ReC$_6$H** (0.226 g, 0.329 mmol), CuI (0.0658 g, 0.345 mmol), and THF (10 mL) and cooled to −45 °C. Then *n*-BuLi (2.4 M in hexane; 0.144 mL, 0.345 mmol) was added with stirring.[61] After 0.5 h, EtNH$_2$ (ca. 1 mL) was added. A solution of BrC≡CC≡CSiEt$_3$ (0.080 g, 0.33 mmol) in THF (5 mL) was added dropwise. After 30 min, solvent was removed by rotary evaporation. The residue was extracted with benzene (3 × 5 mL). The extract was filtered, and solvent was removed by oil pump vacuum. Silica gel column chromatography (20 × 2 cm; benzene) gave a red-brown band. Solvent was removed by oil pump vacuum. Boiling hexane (50 mL) was added. The sample was kept at −90 °C for 24 h. Orange-brown microcrystals were collected by filtration and dried by oil pump vacuum to give **ReC$_{10}$SiEt$_3$** (0.123 g, 0.145 mmol, 44%). DSC (T_i/T_e/T_p):[28] 135/150/183 °C. Anal. Calcd for $C_{44}H_{45}NOPReSi$: C, 62.24; H, 5.34. Found: C, 62.16; H, 5.41. R_f[64] = 0.59. IR (cm^{-1}, THF) $\nu_{C\equiv C}$ 2157 vw, 2132 vw, 2069 w, 2035 vs, 1955 vs, ν_{NO} 1660 s. UV−vis (9.8 × 10^{-6} M):[65] 232 (57 000), 240 sh (54 000), 246 sh (53 000), 270 (55 000), 280 (55 000), 296 (45 000), 330 (33 000), 354 (50 000), 382 (77 000), 430 (8900), 470 (9900), 514 (7700). MS:[66e] 849 (**ReC$_{10}$SiEt$_3^+$**, 100%), 614 (**Re**$^+$, 33%); no other peaks above 300 of >5%.

Procedure B. A Schlenk flask was charged with **ReC$_8$H** (0.0998 g, 0.140 mmol) and THF (5 mL) and cooled to −45 °C. Then *n*-BuLi (2.2 M in hexane; 70 mL, 0.15 mmol) was added with stirring.[61] After 2 h, the cold bath was removed, and CuI (0.0294 g, 0.154 mmol) was added. After 30 min, the mixture was cooled to −20 °C, and EtNH$_2$ (ca. 0.5 mL) was added. A solution of BrC≡CSiEt$_3$ (0.0338 g, 0.154 mmol)[15b] in THF (2 mL) was added dropwise. After 10 min, solvent was removed by oil pump vacuum. The residue was extracted with benzene (2 × 3 mL). The extract was filtered through a 2-cm silica gel pad, and solvent was removed by oil pump vacuum. The residue was extracted with boiling hexane (100 mL). The extract was filtered, and **ReC$_{10}$SiEt$_3$** (0.0306 g, 0.0360 mmol, 26%) was isolated as in procedure A.

Procedure C.[33c] A Schlenk flask was charged with **ReC$_8$H** (0.132 g, 0.186 mmol), *t*-BuOCu (0.0330 g, 0.241 mmol),[69,70] and THF (50 mL). The mixture was stirred for 1 h and cooled to −20 °C. Then EtNH$_2$ (ca. 0.5 mL) was added. A solution of BrC≡CSiEt$_3$ (0.0407 g, 0.186 mmol) in THF (2 mL) was added dropwise. After 0.5 h, the cold bath was removed and solvent was removed by oil pump vacuum. The residue was extracted with toluene (3 × 5 mL). The extract was filtered through a 2-cm silica gel pad, and solvent was removed by oil pump vacuum. The residue was dissolved in THF (ca. 1.5 mL). Silica gel column chromatography (35 × 2 cm; 3:1 v/v hexane/THF) gave a red band. Solvent was removed by oil pump vacuum. The residue was dissolved in a minimum of toluene (ca. 0.3 mL). Hot hexane (30 mL) was added, and **ReC$_{10}$SiEt$_3$** (0.0585 g, 0.0360 mmol, 37%) was isolated as in procedure A.

NMR:[67] ^{1}H (C_6D_6) 7.66−7.52 (m, 6H of 3C$_6$H$_5$), 7.14−6.94 (m, 9H of 3C$_6$H$_5$), 1.52 (s, C$_5$(CH$_3$)$_5$), 0.92 (t, J_{HH} = 8.1, 3CH$_2$C$\underline{H}_3$), 0.47 (q, J_{HH} = 8.1, 3SiC$\underline{H}_2$); ^{13}C{^{1}H} (CD_2Cl_2) 134.5 (*i*-Ph),[68] 134.3 (d, J_{CP} = 10.7, *o*-Ph), 131.1 (d, J_{CP} = 2.4, *p*-Ph), 128.9 (d, J_{CP} = 10.7, *m*-Ph), 122.7 (d, J_{CP} = 15.1, ReC$\underline{C}$), 112.6 (s, ReC$\underline{C}$), 102.2 (s, $\underline{C}_5$(CH$_3$)$_5$), 89.7, 87.1 (2 s, $\underline{CC}$Si), 64.2 (d, J_{CP} = 1.8, ReCC$\underline{C}$), 66.5, 66.5, 65.0, 64.0, 63.0 (5 s, ReCCC$\underline{CCCCC}$), 10.2 (s, C$_5$($\underline{C}$H$_3$)$_5$), 7.7 (s, CH$_2$$\underline{C}H_3$), 4.7 (s, $\underline{C}$H$_2$CH$_3$); ^{31}P{^{1}H} (C_6D_6) 20.8 (s).

ReC$_{12}$SiMe$_3$. A Schlenk flask was charged with **ReC$_8$H** (0.243 g, 0.342 mmol), CuI (0.0652 g, 0.342 mmol), and THF (10 mL) and cooled to −45 °C. Then *n*-BuLi (2.4 M in hexane; 0.14 mL, 0.34 mmol) was added with stirring.[61] After 15 min, EtNH$_2$ (ca. 0.9 mL) was added. A solution of BrC≡CC≡CSiMe$_3$ (0.0688 g, 0.342 mmol)[15a] in THF (5 mL) was added dropwise. The cold bath was removed. After 10 min, solvent was removed by rotary evaporation. The residue was extracted with benzene (3 × 5 mL). The extract was filtered through a 10-cm silica gel column, and solvent was removed by oil pump vacuum. Silica gel column chromatography (35 × 5 cm; 3:1 v/v hexane/THF) gave a brick red band. Solvent was removed by rotary evaporation. The residue was extracted with a minimum of toluene (ca. 5 mL). Hexane (30 mL) was added. The sample was kept at −90 °C for 24 h. The supernatant was decanted (−80 °C), and the red-black microcrystals were dried by oil pump vacuum to give **ReC$_{12}$SiMe$_3$** (0.1220 g, 0.1468 mmol, 43%).[75] R_f[64] = 0.58. DSC (T_i/T_e/T_p):[28] 90/106/140 °C. IR (cm^{-1}, THF): $\nu_{C\equiv C}$ 2136 w, 2074 w, 2016 vs, 1942 vs, ν_{NO} 1660 s. UV−vis (1.9 × 10^{-5} M):[65] 230 (48 000), 280 sh (52 000), 292 (58 000), 306 (59 000), 324 (52 000), 346 (43 000), 386 (53 000), 414 (70 000), 468 (13 000), 508 (14 000), 554 (11 000). MS:[66c] 831 (**ReC$_{12}$SiMe$_3^+$**, 100%), 614 (**Re**$^+$, 23%); no other peaks above 400 of >8%.

NMR:[67] ^{1}H (CD_2Cl_2) 7.58−7.32 (m, 3C$_6$H$_5$), 1.74 (s, C$_5$(CH$_3$)$_5$), 0.19 (s, SiMe$_3$); ^{13}C{^{1}H} (CD_2Cl_2) 134.3 (d, J_{CP} = 11.3, *o*-Ph), 134.0 (*i*-Ph),[68] 131.1 (s, *p*-Ph), 128.9 (d, J_{CP} = 10.5, *m*-Ph), 125.2 (d, J_{CP} = 15.4, ReC$\underline{C}$), 112.9 (s, ReC$\underline{C}$), 102.4 (s, $\underline{C}_5$(CH$_3$)$_5$), 89.2, 88.2 (2 s, $\underline{CC}$Si), 66.0 (d, J_{CP} = 2.4, ReCC$\underline{C}$), 66.2, 65.5, 64.7, 64.5, 64.2, 63.4, 63.0 (7 s, ReCCC$\underline{CCCCCCC}$), 10.2 (s, C$_5$($\underline{C}$H$_3$)$_5$), −0.4 (s, SiCH$_3$); ^{31}P{^{1}H} (CD_2Cl_2/C_6D_6) 22.7/19.6 (s).

ReC$_{20}$Re. Procedure A.[39] A Schlenk flask was charged with **ReC$_{10}$SiMe$_3$** (0.085 g, 0.10 mmol), freshly ground K$_2$CO$_3$ (0.014 g, 0.10 mmol), and MeOH (10 mL). The mixture was stirred vigorously. After 8 h, solvent was removed by oil pump vacuum. The residue was extracted with toluene (2 × 5 mL). The extract was filtered through a 2-cm silica gel pad to give a brown solution of **ReC$_{10}$H**.[74] Pyridine (5 mL) and Cu(OAc)$_2$ (0.018 g, 0.10 mmol) were added. The mixture was stirred at 60 °C for 0.5 h. Solvent was removed by oil pump vacuum. The residue was extracted with THF (2 × 5 mL). The extract was filtered through a 2-cm silica gel pad and concentrated (ca. 2 mL). Silica gel column chromatography (40 × 2 cm; 3:1 → 1:3 v/v hexane/THF) gave a greenish brown band. Solvent was removed by oil pump vacuum. The residue was dissolved in benzene (2 mL). A second column (40 × 2 cm; 3:1 v/v benzene/hexane) gave a dark brown band. Solvent was removed by oil pump vacuum. The residue was dissolved in a minimum of CH_2Cl_2 (2 mL), and hexane (10 mL) was added. A black powder was collected by filtration and dried by oil pump vacuum to give **ReC$_{20}$Re** (0.030 g, 0.020 mmol, 41%).[62,63,75] R_f[64] = 0.31. UV−vis (3.7 × 10^{-6} M):[65] 228 (78 000), 384 sh (110 000), 430/*432* (130 000), 466/*466* (190 000), 508/*510* (140 000), 582/*586* (73 000), 602/*610* (73 000). MS:[66c] 1469 (**ReC$_{20}$Re**$^+$, 100%); no other peaks above 325 of >18%.

(69) Tsuda, T.; Hashimoto, T.; Saegusa, T. *J. Am. Chem. Soc.* **1972**, *94*, 658.

(70) This compound was added in an inert atmosphere glovebox.

(71) This synthesis is based upon methodology reported in the following paper: Hofmeister, H.; Annen, K.; Laurent, H.; Wiechert, R. *Angew. Chem.* **1984**, *96*, 720; *Angew. Chem., Int. Ed. Engl.* **1984**, *23*, 727.

(72) ***Caution***: It has been reported that 1-halobutadiynes can explode upon heating (de Graaf, W.; Smits, A.; Boersma, J.; van Koten, G.; Hoekstra, W. P. M. *Tetrahedron* **1988**, *44*, 6699.). However, we have yet to experience any problems with BrC≡CC≡CSiR$_3$ (R = Me, Et).

(73) This synthesis is based upon methodology reported in the following paper: Nishikawa, T.; Shibuya, S.; Hosokawa, S.; Isobe, M. *Synlett* **1994**, 485.

(74) Data for **ReC$_{10}$H**: IR (cm^{-1}, MeOH/toluene) $\nu_{C\equiv C}$ 2162/2164 w, 2114/2116 w, 2058/2058 m/s, 2028/2031 s/vs, 1960/1962 s/vs, ν_{NO} 1652/1653 vs/s; MS[66b] 735 (**ReC$_{10}$H**$^+$, 100%), 614 (**Re**$^+$, 25%), no other peaks above 460 of >7%; ^{31}P{^{1}H} NMR (C_6D_6)[67] 20.3 (s).

(75) Repeated attempts to obtain correct microanalyses were unsuccessful.

Procedure B. A Schlenk tube was charged with **ReC$_{10}$SiEt$_3$** (0.0300 g, 0.0353 mmol) and toluene (20 mL). Then *n*-$Bu_4N^+F^-$ (1.0 M in THF/5 wt % H_2O; 0.01 mL, 0.01 mmol) was added dropwise with stirring. After 0.5 h, the sample was cannulated into a 50 °C solution of $Cu(OAc)_2$ (0.0083 g, 0.046 mmol) in pyridine (20 mL). After 0.5 h, solvent was removed by oil pump vacuum. The residue was extracted with benzene (3 × 10 mL). The extract was filtered through a 3-cm silica gel pad and concentrated by rotary evaporation (ca. 1 mL). Silica gel column chromatography (25 × 2 cm; benzene) gave a brown-black band. Solvent was removed by oil pump vacuum. The residue was dissolved in a minimum of CH_2Cl_2 (ca. 1 mL), and hexane (5 mL) was added. A black powder was collected by filtration and dried by oil pump vacuum to give **ReC$_{20}$Re** (0.0134 g, 0.00912 mmol, 52%).[75]

NMR:[67] ^{1}H (THF-d_8) 7.57−7.48 (m, 12H of 6C_6H_5), 7.47−7.40 (m, 18H of 6C_6H_5), 1.77 (s, 2$C_5(CH_3)_5$); ^{13}C{^{1}H} (CD_2Cl_2) 134.3 (d, J_{CP} = 11.0, *o*-Ph), 131.1 (s, *p*-Ph), 129.0 (d, J_{CP} = 10.6, *m*-Ph),[68] 127.3 (d, J_{CP} = 14.6, Re$\underline{C}$C), 113.2 (s, ReC$\underline{C}$), 102.5 (s, $\underline{C}_5(CH_3)_5$), 66.6 (ReC$\underline{C}$), 67.0, 66.5, 65.5, 65.4, 65.3, 64.9, 64.8 (7 s, ReC-C$\underline{CCCCCCC}$), 10.2 (s, $C_5(\underline{C}H_3)_5$); ^{31}P{^{1}H} (C_6D_6/THF-d_8) 20.2/21.7 (s).

HC≡CC≡CSiEt$_3$.[8] A Schlenk flask was charged with $Et_3SiC{\equiv}CC{\equiv}CSiEt_3$ (8.475 g, 30.42 mmol)[8] and ether (100 mL). Then MeLi·LiBr (1.0 M in ether; 36.5 mL, 36.5 mmol) was added with stirring. After 24 h, the dark green mixture was slowly poured into saturated aqueous NH_4Cl (200 mL, 0 °C). The aqueous layer was extracted with pentane (3 × 50 mL). The combined organic layers were dried (Na_2SO_4). Solvents were removed by rotary evaporation below room temperature (ice water bath). The residue was vacuum transferred to give $HC{\equiv}CC{\equiv}CSiEt_3$ as a colorless liquid (2.615 g, 15.91 mmol, 52%) that was stored in a freezer. IR (cm^{-1}, ether): $\nu_{C\equiv C}$ 2187 vs, 2033 s.

NMR ($CDCl_3$):[67] ^{1}H 2.06 (s, HC≡), 0.98 (t, J_{HH} = 7.8, CH_3), 0.61 (q, J_{HH} = 7.8, CH_2); ^{13}C{^{1}H} 88.6 (s, $\underline{C}$CSi), 83.1 (s, C$\underline{C}$Si), 68.7 (s, H$\underline{C}$C), 66.2 (s, HC$\underline{C}$), 7.6 (s, CH_3), 4.3 (s, CH_2).

BrC≡CC≡CSiEt$_3$.[38,71,72] A round-bottom flask was charged with $HC{\equiv}CC{\equiv}CSiEt_3$ (2.03 g, 12.3 mmol), $AgNO_3$ (0.629 g, 3.70 mmol), and acetone (100 mL). The mixture was stirred. After 10 min, NBS (2.42 g, 13.6 mmol) was added. After 8 h, pentane (100 mL) was added. The mixture was filtered, and the flask was rinsed with pentane (2 × 10 mL). Ice water (40 mL) was poured onto the combined filtrates with stirring. The aqueous layer was extracted with pentane (2 × 20 mL). The combined organic layers were dried (Na_2SO_4). Solvents were removed by rotary evaporation (ice water bath). The residue was distilled by oil pump vacuum (49 °C, 0.1 mmHg) to give $BrC{\equiv}CC{\equiv}CSiEt_3$ as a colorless liquid (1.63 g, 6.71 mmol, 54%) that was stored in a freezer. IR (cm^{-1}, film/ether/THF): $\nu_{C\equiv C}$ 2172/2175/2172 vs/s/s, 2091/2093/2091 m.

NMR (C_6D_6):[67] ^{1}H 0.94 (t, J_{HH} = 7.82, 9H, CH_3), 0.49 (q, J_{HH} = 7.89, 6H, CH_2); ^{13}C{^{1}H} 90.4 (s, $\underline{C}$CSi), 82.2 (s, C$\underline{C}$Si; m without ^{1}H decoupling), 67.1 (s, BrC$\underline{C}$), 40.9 (s, Br$\underline{C}$C), 7.88 (s, CH_3; qt without ^{1}H decoupling, $^1J_{CH}$ = 126.4, $^2J_{CH}$ = 4.9), 4.73 (s, CH_2; tm without ^{1}H decoupling, $^1J_{CH}$ = 119.9).

BrC≡CC≡CBr.[36,73] A Schlenk flask was charged with $Me_3SiC{\equiv}CC{\equiv}CSiMe_3$ (5.00 g, 25.7 mmol) and acetone (150 mL) and wrapped with Al foil (light shield). Then $AgNO_3$ (2.20 g, 13.0 mmol) and NBS (18.5 g, 104 mmol) were added with stirring. After 15 h, saturated aqueous NH_4Cl (500 mL) was added. The water layer was extracted with pentane (5 × 50 mL). The combined organic layers were dried (Na_2SO_4). Solvent was removed by rotary evaporation (ice water bath) to give a brown residue that was immediately extracted with pentane. The extract was filtered through a 2-cm silica gel pad and kept at −90 °C for 15 h. Long white needles were isolated by pipeting (or decanting) the supernate and a denser yellow liquid at the bottom the flask. These were washed with cold pentane and dried by oil pump vacuum (<0 °C) to give BrC≡CC≡CBr (0.93 g, 4.5 mmol, 17%), mp 51.5−52.0 °C. The product rapidly decomposes at room temperature but can be stored at −30 °C (stock solution or slowly discoloring needles). IR (cm^{-1}, THF): $\nu_{C\equiv C}$ 2121 vs. MS (EI, 70 eV): 208 (M^+, 100%).

NMR (C_6D_6):[67] ^{13}C{^{1}H} 66.7 (s, $\underline{C}$CBr), 39.0 (s, C$\underline{C}$Br).

Acknowledgment. We thank the NSF for support of this research, and Drs. W. Weng, J. Seyler, and D. Rende for exploratory experiments.

Supporting Information Available: Additional experimental procedures (see text), tables of IR and ^{13}C NMR data (**ReC$_x$H, ReC$_x$SiR$_3$**), and representative IR and Raman spectra (PDF). This material is available free of charge via the Internet at http://pubs.acs.org.

JA992747Z